

Development, Implementation, and Application of an Analytic Second Derivative Formalism for the Normalized Elimination of the Small Component Method

Wenli Zou,[†] Michael Filatov,^{*,‡} and Dieter Cremer^{*,†}

[†]Department of Chemistry, Southern Methodist University, 3215 Daniel Ave, Dallas, Texas 75275-0314, United States

[‡]Mulliken Center for Theoretical Chemistry, Institut für Physikalische und Theoretische Chemie, Universität Bonn, Beringstr. 4, D-53115 Bonn, Germany

ABSTRACT: Analytical second derivatives for the normalized elimination of the small component (NESC) method are derived for the first time and implemented for the routine calculation of NESC vibrational frequencies and other second order molecular properties using the scalar relativistic form of NESC. Using response theory, the second derivatives of the transformation matrix *U* connecting the large and the pseudolarge components of the relativistic wave function are correctly derived. The 24 derivative terms involving the NESC Hamiltonian and the NESC renormalization matrix are individually tested, and their contributions to the energy Hessian are calculated. The influence of a finite nucleus model and that of the picture change is determined. Different ways of speeding up the calculation of the NESC second derivatives are tested. It is shown that second order properties can routinely be calculated in combination with Hartree–Fock, density functional theory, Moller–Plesset perturbation theory, and any other electron correlation corrected quantum chemical method provided analytic second derivatives are available in the nonrelativistic case. The general applicability of the analytic NESC Hessian is demonstrated by benchmark calculations for NESC/DFT calculations involving up to 1500 basis functions.

1. INTRODUCTION

One of the most important applications of the all-electron relativistic quantum chemical methodology is the calculation of molecular properties.¹ The availability of analytic first and second derivatives of the energy is a prerequisite for the analytic evaluation of first and second order molecular response properties. In the domain of many-body quantum mechanics, the use of analytic energy gradients and Hessians is regarded as the preferred way of obtaining molecular properties.² Furthermore, there is a general consensus that the analytic techniques of calculating energy derivatives are significantly more efficient and more precise than the numeric or seminumeric differentiation methods.²

The second derivatives of the energy with regard to the nuclear displacements (thus yielding the energy Hessian) are required to calculate the vibrational frequencies of a molecule. This implies that all of the molecular integrals and the molecular orbital (MO) coefficients are differentiated. The analytic molecular Hessian formalism can be combined with the appropriate molecular integral derivatives for obtaining also other molecular response properties such as electric polarizabilities, infrared intensities, magnetic susceptibilities, magnetic shielding tensors, indirect nuclear spin–spin coupling constants, etc. In its own right, the Hessian matrix plays an important role for characterizing the molecular potential energy surfaces (PESs) whereby its eigenvalues characterize stationary points as minima, first order, or higher order saddle points. Furthermore, they determine the curvature of a PES at a stationary point and by this the vibrational force constants of a molecule, which, by solving the basic equation of vibrational spectroscopy, lead to the molecular vibrational frequencies. These in turn are needed to calculate zero-point energies and

vibrational contributions to the enthalpy and entropy at a given temperature.

Recently, we have started a multistep-development task with the purpose of increasing the applicability of the normalized elimination of the small component (NESC) method³ in its scalar relativistic form by deriving analytic energy derivatives for the routine calculation of response properties. Among the exact two-component all-electron relativistic approaches, the NESC method, which was originally derived by Dyall,³ represents perhaps the most concise and efficient computational scheme that enables one to obtain relativistically corrected molecular energies at the cost of a nonrelativistic quantum chemical calculation.^{3–7} Dyall's pioneering work^{3,5} triggered related developments such as, for example, the work by Filatov and others.^{6,8,9} Systematic applications of NESC were carried out by Cremer and co-workers,^{10,11} Kraka and Cremer,¹² and Filatov and co-workers.^{13–17} NESC was also, directly or indirectly, relevant for the development work on the infinite order Douglas–Kroll–Hess (IODKH) method,^{18–21} the matrix driven formulation of the infinite order two-component (IOTC) method,^{22–24} the X2C method,^{25–27} or the calculation of relativistically corrected molecular properties.^{28,29}

In recent work, we have derived analytic energy derivatives for the routine optimization of molecular geometries³⁰ and the calculation of other first order molecular response properties. The NESC first derivative formalism³⁰ has been developed and applied to the analytic calculation of effective contact densities needed for the calculation of Mössbauer isomer shifts,³¹ hyperfine structure constants of paramagnetic molecules,³²

Received: February 11, 2012

Published: July 10, 2012



and electric field gradients at the nuclear site.³³ In this work, we will extend the applicability spectrum of NESC by deriving, implementing, and employing the methodology of analytic second derivatives with respect to nuclear displacements. Although we will focus on the molecular Hessian and vibrational frequencies, our intention is to derive and implement a general analytic second derivative formalism, which can be used for obtaining relativistically corrected second order molecular response properties such as molecular polarizabilities, infrared intensities, magnetic shieldings, or indirect nuclear spin–spin coupling constants.

The theory of the analytic NESC second derivatives is presented in sections 2–4. When deriving analytic derivatives in the context of exact two-component relativistic methods, such as NESC, the major difficulty originates from the necessity of differentiating matrices of operators, which cannot be expressed in a concise analytic form, which is the case for the elimination of the small component operator of NESC. Analytic derivatives of this operator as well as of the renormalization matrix of NESC are derived in detail in Appendices A–C. In section 5, the implementation of the NESC second derivatives and details of the computations using the formalism derived are described. The results of the Hessian and vibrational frequencies calculations are presented in section 6, where the accuracy and feasibility of the NESC second derivative formalism is analyzed by comparison with the results of other calculations and experimental data. Conclusions are presented in the final section.

2. THE NESC METHOD

Starting from the four-component Dirac equation with embedded restricted kinetic balance (RKB):

$$\begin{pmatrix} \mathbf{V} & \mathbf{T} \\ \mathbf{T} & \mathbf{W} - \mathbf{T} \end{pmatrix} \begin{pmatrix} \mathbf{A}_- & \mathbf{A}_+ \\ \mathbf{B}_- & \mathbf{B}_+ \end{pmatrix} = \begin{pmatrix} \mathbf{S} & \mathbf{0} \\ \mathbf{0} & \frac{1}{2mc^2} \mathbf{T} \end{pmatrix} \begin{pmatrix} \mathbf{A}_- & \mathbf{A}_+ \\ \mathbf{B}_- & \mathbf{B}_+ \end{pmatrix} \begin{pmatrix} \boldsymbol{\varepsilon}_- & \mathbf{0} \\ \mathbf{0} & \boldsymbol{\varepsilon}_+ \end{pmatrix} \quad (1)$$

Dyall obtained the NESC equation³

$$\tilde{\mathbf{L}}\mathbf{A}_+ = \tilde{\mathbf{S}}\mathbf{A}_+\boldsymbol{\varepsilon}_+ \quad (2)$$

by (i) eliminating the positronic eigenvalues $\boldsymbol{\varepsilon}_-$ as well as the corresponding eigenvectors \mathbf{A}_- and \mathbf{B}_- and (ii) introducing a matrix \mathbf{U} , which connects the large component \mathbf{A}_+ and the pseudolarge component \mathbf{B}_+ via

$$\mathbf{B}_+ = \mathbf{U}\mathbf{A}_+ \quad (3)$$

In eq 2, the relativistic metric is given by eq 4.

$$\tilde{\mathbf{S}} = \mathbf{S} + \frac{1}{2mc^2} \mathbf{U}^\dagger \mathbf{T} \mathbf{U} \quad (4)$$

In eq 1, \mathbf{S} , \mathbf{T} , and \mathbf{V} are the matrices of the overlap, kinetic energy, and potential energy operators, and \mathbf{W} is the matrix of the operator $1/(4m^2c^2)(\boldsymbol{\sigma} \cdot \mathbf{p})V(\mathbf{r})(\boldsymbol{\sigma} \cdot \mathbf{p})$ (or $1/(4m^2c^2)\nabla V(\mathbf{r}) \cdot \nabla$ in the scalar relativistic approximation) in the basis of the atomic orbitals $\chi_\mu(\mathbf{r})$.³

The NESC Hamiltonian $\tilde{\mathbf{L}}$ takes the form

$$\tilde{\mathbf{L}} = \tilde{\mathbf{T}} + \tilde{\mathbf{V}} \quad (5)$$

where $\tilde{\mathbf{T}}$ and $\tilde{\mathbf{V}}$ are defined as in eqs 6 and 7, respectively:

$$\tilde{\mathbf{T}} = \mathbf{U}^\dagger \mathbf{T} + \mathbf{T} \mathbf{U} - \mathbf{U}^\dagger \mathbf{T} \mathbf{U} \quad (6)$$

$$\tilde{\mathbf{V}} = \mathbf{V} + \mathbf{U}^\dagger \mathbf{W} \mathbf{U} \quad (7)$$

Matrix \mathbf{U} can be calculated either iteratively using one of the following equations

$$\mathbf{U} = \mathbf{T}^{-1}(\tilde{\mathbf{S}}\tilde{\mathbf{L}} - \mathbf{V}) \quad (8)$$

$$= (\mathbf{T} - \mathbf{W})^{-1} \mathbf{T} \left[\mathbf{I} - \frac{1}{2mc^2} \mathbf{U} \mathbf{S}^{-1} (\mathbf{T} \mathbf{U} + \mathbf{V}) \right] \quad (9)$$

or in a one-step noniterative method.⁷ In the following, all derivations are carried out in the scalar relativistic form.

In the case of a many-electron problem described for example by the Hartree–Fock or Kohn–Sham method, the one-electron NESC Hamiltonian $\tilde{\mathbf{L}}$ can be renormalized on the nonrelativistic metric

$$\mathbf{H}_{1-e} = \mathbf{G}^\dagger \tilde{\mathbf{L}} \mathbf{G} \quad (10)$$

and used in connection with the nonrelativistic energy expression.⁵ In eq 10, matrix \mathbf{G} is the renormalization matrix:³⁴

$$\mathbf{G} = \mathbf{S}^{-1/2} (\mathbf{S}^{-1/2} \tilde{\mathbf{S}} \mathbf{S}^{-1/2})^{-1/2} \mathbf{S}^{1/2} \quad (11)$$

implying that

$$\mathbf{G} \mathbf{G} = \tilde{\mathbf{S}}^{-1} \mathbf{S} \quad (12)$$

The renormalization matrix is positive definite, which is of relevance for the calculation of its derivatives (see Appendix A). The Fock matrix is then defined by

$$\mathbf{F} = \mathbf{H}_{1-e} + (\mathbf{J} - \mathbf{K}) \quad (13)$$

and the total electronic energy E of the many-electron system by eq 14,

$$E = \text{tr} \mathbf{P} \mathbf{H}_{1-e} + \frac{1}{2} \text{tr} \mathbf{P} (\mathbf{J} - \mathbf{K}) \quad (14)$$

where \mathbf{J} and \mathbf{K} are the Coulomb and exchange parts of the Fock matrix and \mathbf{P} is the density matrix calculated as $\mathbf{P} = \mathbf{C} \mathbf{n} \mathbf{C}^\dagger$. There, diagonal matrix \mathbf{n} contains the orbital occupation numbers, and matrix \mathbf{C} collects the eigenvectors of the Fock matrix obtained from diagonalization of the pseudoeigenvalue problem (eq 15):

$$\mathbf{F} \mathbf{C} = \mathbf{S} \mathbf{C} \boldsymbol{\varepsilon} \quad (15)$$

3. ANALYTIC GRADIENT OF THE NESC ENERGY

Taking a derivative of the electronic energy (eq 14) with regard to λ , where λ corresponds, for example, to a nuclear coordinate or to a component of the electric field, one obtains the analytic gradient of E :

$$\frac{\partial E}{\partial \lambda} = \text{tr} \mathbf{\Omega} \frac{\partial \mathbf{S}}{\partial \lambda} + \text{tr} \mathbf{P} \frac{\partial \mathbf{H}_{1-e}}{\partial \lambda} + \frac{1}{2} \text{tr} \mathbf{P} \frac{\partial'}{\partial \lambda} (\mathbf{J} - \mathbf{K}) \quad (16)$$

Here, matrix $\mathbf{\Omega}$ is defined by $\mathbf{\Omega} = -\mathbf{C} \boldsymbol{\varepsilon} \mathbf{n} \mathbf{C}^\dagger$, and the prime at $\partial'/\partial \lambda$ implies that only the two-electron integrals rather than the density matrix need to be differentiated. The first and the last term on the right-hand side (rhs) are calculated utilizing nonrelativistic methodology. Only, the second term has to be determined in a NESC gradient calculation.

Writing the derivative of the renormalized NESC Hamiltonian as

$$\frac{\partial \mathbf{H}_{1-e}}{\partial \lambda} = \frac{\partial \mathbf{G}^\dagger}{\partial \lambda} \tilde{\mathbf{L}} \mathbf{G} + \mathbf{G}^\dagger \tilde{\mathbf{L}} \frac{\partial \mathbf{G}}{\partial \lambda} + \mathbf{G}^\dagger \frac{\partial \tilde{\mathbf{L}}}{\partial \lambda} \mathbf{G} \quad (17)$$

the second term in eq 16 adopts the form

$$tr \mathbf{P} \frac{\partial \mathbf{H}_{1-e}}{\partial \lambda} = tr \tilde{\mathbf{P}} \frac{\partial \tilde{\mathbf{L}}}{\partial \lambda} + tr \mathbf{D} \frac{\partial \mathbf{G}^\dagger}{\partial \lambda} + tr \mathbf{D}^\dagger \frac{\partial \mathbf{G}}{\partial \lambda} \quad (18)$$

where the new matrices $\tilde{\mathbf{P}} = \mathbf{G} \mathbf{P} \mathbf{G}^\dagger$ and $\mathbf{D} = \tilde{\mathbf{L}} \mathbf{G} \mathbf{P}$ are introduced.

The derivatives of the matrix $\tilde{\mathbf{L}}$ are obtained by differentiating eqs 5, 6, and 7,

$$\begin{aligned} \frac{\partial \tilde{\mathbf{L}}}{\partial \lambda} &= \mathbf{U}^\dagger \frac{\partial \mathbf{T}}{\partial \lambda} + \frac{\partial \mathbf{T}}{\partial \lambda} \mathbf{U} - \mathbf{U}^\dagger \frac{\partial \mathbf{T}}{\partial \lambda} \mathbf{U} + \mathbf{U}^\dagger \frac{\partial \mathbf{W}}{\partial \lambda} \mathbf{U} \\ &+ \frac{\partial \mathbf{V}}{\partial \lambda} + \frac{\partial \mathbf{U}^\dagger}{\partial \lambda} [\mathbf{T} - (\mathbf{T} - \mathbf{W}) \mathbf{U}] \\ &+ [\mathbf{T} - \mathbf{U}^\dagger (\mathbf{T} - \mathbf{W})] \frac{\partial \mathbf{U}}{\partial \lambda} \end{aligned} \quad (19)$$

Then, the first term on the rhs of eq 18 can be calculated by

$$\begin{aligned} tr \tilde{\mathbf{P}} \frac{\partial \tilde{\mathbf{L}}}{\partial \lambda} &= tr(\mathbf{U} \tilde{\mathbf{P}} + \tilde{\mathbf{P}} \mathbf{U}^\dagger - \mathbf{U} \tilde{\mathbf{P}} \mathbf{U}^\dagger) \frac{\partial \mathbf{T}}{\partial \lambda} + tr(\mathbf{U} \tilde{\mathbf{P}} \mathbf{U}^\dagger) \frac{\partial \mathbf{W}}{\partial \lambda} \\ &+ tr \tilde{\mathbf{P}} \frac{\partial \mathbf{V}}{\partial \lambda} + tr \left(\mathbf{P}_0^\dagger \frac{\partial \mathbf{U}^\dagger}{\partial \lambda} + \mathbf{P}_0 \frac{\partial \mathbf{U}}{\partial \lambda} \right) \end{aligned} \quad (20)$$

where $\mathbf{P}_0 = \tilde{\mathbf{P}}(\mathbf{T} - \mathbf{U}^\dagger(\mathbf{T} - \mathbf{W}))$. For the first three terms on the rhs of eq 20, the one-electron integral derivatives are directly available from nonrelativistic quantum chemical codes. The major difficulty, when evaluating eqs 18 and 20, originates from the terms containing the derivatives $\partial \mathbf{U} / \partial \lambda$ of the elimination of the small component operator \mathbf{U} (see, eqs 3, 8, and 9) and the derivatives $\partial \mathbf{G} / \partial \lambda$ of the renormalization matrix \mathbf{G} (eq 11). The exact expressions for obtaining these derivatives have been derived in our previous publications^{30,31} (see also Appendices A and B where the new formulas for the second derivatives of these matrices are given).

4. ANALYTIC SECOND DERIVATIVES OF THE NESC ENERGY

Starting from eq 16, the second derivatives can be calculated as

$$\begin{aligned} \frac{\partial^2 E}{\partial \mu \partial \lambda} &= tr \mathbf{\Omega} \frac{\partial^2 \mathbf{S}}{\partial \mu \partial \lambda} + tr \mathbf{P} \frac{\partial^2 \mathbf{H}_{1-e}}{\partial \mu \partial \lambda} + \frac{1}{2} tr \mathbf{P} \frac{\partial^2}{\partial \mu \partial \lambda} (\mathbf{J} - \mathbf{K}) \\ &+ tr \frac{\partial \mathbf{\Omega}}{\partial \mu} \frac{\partial \mathbf{S}}{\partial \lambda} + tr \frac{\partial \mathbf{P}}{\partial \mu} \frac{\partial \mathbf{H}_{1-e}}{\partial \lambda} + \frac{1}{2} tr \frac{\partial \mathbf{P}}{\partial \mu} \frac{\partial}{\partial \lambda} (\mathbf{J} - \mathbf{K}) \end{aligned} \quad (21)$$

The first and the third terms in eq 21 are calculated utilizing the standard nonrelativistic methodology. The derivatives $\partial \mathbf{P} / \partial \mu$ and $\partial \mathbf{\Omega} / \partial \mu$ are obtained from the coupled perturbed (CP) equations,^{2,35} which employ the derivatives $\partial \mathbf{H}_{1-e} / \partial \mu$. The NESC CP equations are presented in Appendix C.

For the second to last term of eq 21, the derivative matrix $\partial \mathbf{H}_{1-e} / \partial \lambda$ is given in eqs 17 and 19. By differentiating eq 17 another time, one obtains the second derivative of the renormalized NESC Hamiltonian and thereby also the second term in eq 21:

$$\begin{aligned} \frac{\partial^2 \mathbf{H}_{1-e}}{\partial \mu \partial \lambda} &= \frac{\partial^2 \mathbf{G}^\dagger}{\partial \mu \partial \lambda} \tilde{\mathbf{L}} \mathbf{G} + \mathbf{G}^\dagger \tilde{\mathbf{L}} \frac{\partial^2 \mathbf{G}}{\partial \mu \partial \lambda} + \mathbf{G}^\dagger \frac{\partial^2 \tilde{\mathbf{L}}}{\partial \mu \partial \lambda} \mathbf{G} \\ &+ \frac{\partial \mathbf{G}^\dagger}{\partial \mu} \tilde{\mathbf{L}} \frac{\partial \mathbf{G}}{\partial \lambda} + \frac{\partial \mathbf{G}^\dagger}{\partial \lambda} \tilde{\mathbf{L}} \frac{\partial \mathbf{G}}{\partial \mu} + \frac{\partial \mathbf{G}^\dagger}{\partial \mu} \frac{\partial \tilde{\mathbf{L}}}{\partial \lambda} \mathbf{G} \\ &+ \frac{\partial \mathbf{G}^\dagger}{\partial \lambda} \frac{\partial \tilde{\mathbf{L}}}{\partial \mu} \mathbf{G} + \mathbf{G}^\dagger \frac{\partial \tilde{\mathbf{L}}}{\partial \lambda} \frac{\partial \mathbf{G}}{\partial \mu} + \mathbf{G}^\dagger \frac{\partial \tilde{\mathbf{L}}}{\partial \mu} \frac{\partial \mathbf{G}}{\partial \lambda} \end{aligned} \quad (22)$$

$$\begin{aligned} tr \mathbf{P} \frac{\partial^2 \mathbf{H}_{1-e}}{\partial \mu \partial \lambda} &= tr \tilde{\mathbf{P}} \frac{\partial^2 \tilde{\mathbf{L}}}{\partial \mu \partial \lambda} + tr \left(\mathbf{D} \frac{\partial^2 \mathbf{G}^\dagger}{\partial \mu \partial \lambda} + \mathbf{D}^\dagger \frac{\partial^2 \mathbf{G}}{\partial \mu \partial \lambda} \right) \\ &+ tr \mathbf{P} \left[\left(\frac{\partial \mathbf{G}^\dagger}{\partial \mu} \frac{\partial \tilde{\mathbf{L}}}{\partial \lambda} + \frac{\partial \mathbf{G}^\dagger}{\partial \lambda} \frac{\partial \tilde{\mathbf{L}}}{\partial \mu} \right) \mathbf{G} \right. \\ &+ \left. \mathbf{G}^\dagger \left(\frac{\partial \tilde{\mathbf{L}}}{\partial \lambda} \frac{\partial \mathbf{G}}{\partial \mu} + \frac{\partial \tilde{\mathbf{L}}}{\partial \mu} \frac{\partial \mathbf{G}}{\partial \lambda} \right) \right] \\ &+ tr \mathbf{P} \left(\frac{\partial \mathbf{G}^\dagger}{\partial \mu} \tilde{\mathbf{L}} \frac{\partial \mathbf{G}}{\partial \lambda} + \frac{\partial \mathbf{G}^\dagger}{\partial \lambda} \tilde{\mathbf{L}} \frac{\partial \mathbf{G}}{\partial \mu} \right) \end{aligned} \quad (23)$$

In eq 23, the first and second derivatives of matrix \mathbf{G} can be calculated using the methods described in Appendix A. Note, however, that the derivatives of the elements of the renormalization matrix \mathbf{G} with respect to the nuclear displacements are very small, on the order of 10^{-4} a.u. or less. Indeed, the renormalization matrix \mathbf{G} is sufficiently close to a unit matrix (see eq 12) for all of the basis functions except for the tightest ones. For the latter basis functions, however, the dependence of the matrix elements of \mathbf{G} on the molecular geometry is the weakest. Consequently, the contribution of the last term of eq 23 is on the order of 10^{-7} a.u. or less (see Table 1). Hence, this term can be neglected for the calculation of vibrational frequencies.

The expression for $\partial \tilde{\mathbf{L}} / \partial \lambda$ in the third term of eq 23 is given in eq 19 where the terms containing the $\partial \mathbf{U} / \partial \lambda$ derivatives can be neglected on the basis of their magnitude. As discussed in refs 31–33, these terms make negligibly small contributions to the energy derivatives, even when calculating the properties strongly dependent on the core electrons, such as the contact densities or isotropic hyperfine structure constants. A further simplification of the third term of eq 23 originates from the observation that the contributions from $\partial \mathbf{V} / \partial \lambda$ in eq 19 are usually 10^3 times greater than those from $\partial \mathbf{T} / \partial \lambda$ and $\partial \mathbf{W} / \partial \lambda$, respectively. Therefore, for the purpose of calculating geometric derivatives, $\partial \tilde{\mathbf{L}} / \partial \lambda$ in the third term of eq 23 can be replaced by $\partial \mathbf{V} / \partial \lambda$ without leading to any significant errors. The simplifications described are only valid for the NESC derivatives with regard to nuclear coordinates; i.e., when differentiating with respect to other external perturbations, these terms may need to be retained.

Differentiating eq 19 again, one obtains eq 24:

Table 1. Individual Contributions of the Terms in eqs 23–30^a

	AuH	Au ₂	Hg ₂
term 4 in eq 23	-1.2×10^{-6}	-4.7×10^{-7}	-1.4×10^{-8}
eq 26	3.6×10^{-5}	4.5×10^{-5}	6.5×10^{-6}
eq 27	2.0×10^{-5}	1.3×10^{-5}	2.5×10^{-6}
eq 28	-1.6×10^{-5}	-4.9×10^{-6}	2.0×10^{-6}
eq 29	-1.2×10^{-5}	-1.2×10^{-5}	-3.8×10^{-7}
terms T_n in eq 30			
T 2: pc - fn ^b	1.0×10^{-8}	-7.6×10^{-9}	-1.8×10^{-13}
T 3: pc - fn ^c	3.2×10^{-7}	-9.0×10^{-10}	1.0×10^{-11}
T 4: NR - NESC ^d	-0.03231	-0.04970	-0.001738
T 4: AR - NESC ^e	-0.00163	0.00004	0.000010
T 5	0.02448	0.03484	0.001348
T 6	-0.02413	-0.03496	-0.001266
T 6: appr - exact ^f	-0.00004	-0.00001	0.000000
T5 + T6	0.00035	-0.00012	-0.000082
k_e	0.39580	0.23871	0.003429
ω_e (ana.)	2283.7	179.0	21.18
ω_e (num.)	2283.8	178.9	21.1 ± 0.4
ω_e (nonrelat.)	1599.0	121.5	30.7

^aEnergies in hartrees, frequencies in cm⁻¹. See text for more detail.^bDifference between point charge (pc) and finite nucleus (fn) model used in connection with $\partial^2 \mathbf{W} / \partial \mu \partial \lambda$ of term 2. ^cDifference between point charge (pc) and finite nucleus (fn) model used in connection with $\partial^2 \mathbf{V} / \partial \mu \partial \lambda$ of term 3. ^dDifference between nonrelativistic (NR) and relativistic NESC one-electron contribution $\partial \mathbf{H}_{1-e} / \partial \lambda$ in term 4. ^eDifference between approximate relativistic (AR: in term 4 of eq 30, the two $\partial \mathbf{G} / \partial \lambda$ containing contributions are neglected) and exact relativistic NESC one-electron contribution $\partial \mathbf{H}_{1-e} / \partial \lambda$ in term 4. ^fDifference between the approximate (appr) ($\partial \tilde{\mathbf{L}} / \partial \lambda$ is replaced by $\partial \mathbf{V} / \partial \lambda$) and exact description of term 6.

$$\begin{aligned}
\frac{\partial^2 \tilde{\mathbf{L}}}{\partial \mu \partial \lambda} = & \frac{\partial^2 \mathbf{T}}{\partial \mu \partial \lambda} \mathbf{U} + \mathbf{U}^\dagger \frac{\partial^2 \mathbf{T}}{\partial \mu \partial \lambda} - \mathbf{U}^\dagger \left(\frac{\partial^2 \mathbf{T}}{\partial \mu \partial \lambda} - \frac{\partial^2 \mathbf{W}}{\partial \mu \partial \lambda} \right) \mathbf{U} \\
& + \frac{\partial^2 \mathbf{V}}{\partial \mu \partial \lambda} + \frac{\partial^2 \mathbf{U}^\dagger}{\partial \mu \partial \lambda} [\mathbf{T} - (\mathbf{T} - \mathbf{W}) \mathbf{U}] \\
& + [\mathbf{T} - \mathbf{U}^\dagger (\mathbf{T} - \mathbf{W})] \frac{\partial^2 \mathbf{U}}{\partial \mu \partial \lambda} + (\mathbf{I} - \mathbf{U}^\dagger) \\
& \left(\frac{\partial \mathbf{T}}{\partial \mu} \frac{\partial \mathbf{U}}{\partial \lambda} + \frac{\partial \mathbf{T}}{\partial \lambda} \frac{\partial \mathbf{U}}{\partial \mu} \right) + \left(\frac{\partial \mathbf{U}^\dagger}{\partial \lambda} \frac{\partial \mathbf{T}}{\partial \mu} + \frac{\partial \mathbf{U}^\dagger}{\partial \mu} \frac{\partial \mathbf{T}}{\partial \lambda} \right) \\
& (\mathbf{I} - \mathbf{U}) + \mathbf{U}^\dagger \left(\frac{\partial \mathbf{W}}{\partial \mu} \frac{\partial \mathbf{U}}{\partial \lambda} + \frac{\partial \mathbf{W}}{\partial \lambda} \frac{\partial \mathbf{U}}{\partial \mu} \right) \\
& + \left(\frac{\partial \mathbf{U}^\dagger}{\partial \lambda} \frac{\partial \mathbf{W}}{\partial \mu} + \frac{\partial \mathbf{U}^\dagger}{\partial \mu} \frac{\partial \mathbf{W}}{\partial \lambda} \right) \mathbf{U} - \frac{\partial \mathbf{U}^\dagger}{\partial \mu} (\mathbf{T} - \mathbf{W}) \frac{\partial \mathbf{U}}{\partial \lambda} \\
& - \frac{\partial \mathbf{U}^\dagger}{\partial \lambda} (\mathbf{T} - \mathbf{W}) \frac{\partial \mathbf{U}}{\partial \mu}
\end{aligned} \quad (24)$$

such that the first term on the rhs of eq 23 is given by

$$\begin{aligned}
tr \tilde{\mathbf{P}} \frac{\partial^2 \tilde{\mathbf{L}}}{\partial \mu \partial \lambda} = & tr(\mathbf{U} \tilde{\mathbf{P}} + \tilde{\mathbf{P}} \mathbf{U}^\dagger - \mathbf{U} \tilde{\mathbf{P}} \mathbf{U}^\dagger) \frac{\partial^2 \mathbf{T}}{\partial \mu \partial \lambda} \\
& + tr(\mathbf{U} \tilde{\mathbf{P}} \mathbf{U}^\dagger) \frac{\partial^2 \mathbf{W}}{\partial \mu \partial \lambda} + tr \tilde{\mathbf{P}} \frac{\partial^2 \mathbf{V}}{\partial \mu \partial \lambda}
\end{aligned} \quad (25)$$

$$\begin{aligned}
& + tr[\mathbf{T} - (\mathbf{T} - \mathbf{W}) \mathbf{U}] \tilde{\mathbf{P}} \frac{\partial^2 \mathbf{U}^\dagger}{\partial \mu \partial \lambda} + tr \tilde{\mathbf{P}} [\mathbf{T} - \mathbf{U}^\dagger (\mathbf{T} - \mathbf{W})] \\
& \frac{\partial^2 \mathbf{U}}{\partial \mu \partial \lambda}
\end{aligned} \quad (26)$$

$$\begin{aligned}
& + tr \tilde{\mathbf{P}} (\mathbf{I} - \mathbf{U}^\dagger) \left(\frac{\partial \mathbf{T}}{\partial \mu} \frac{\partial \mathbf{U}}{\partial \lambda} + \frac{\partial \mathbf{T}}{\partial \lambda} \frac{\partial \mathbf{U}}{\partial \mu} \right) + tr(\mathbf{I} - \mathbf{U}) \tilde{\mathbf{P}} \\
& \left(\frac{\partial \mathbf{U}^\dagger}{\partial \lambda} \frac{\partial \mathbf{T}}{\partial \mu} + \frac{\partial \mathbf{U}^\dagger}{\partial \mu} \frac{\partial \mathbf{T}}{\partial \lambda} \right)
\end{aligned} \quad (27)$$

$$\begin{aligned}
& + tr \tilde{\mathbf{P}} \mathbf{U}^\dagger \left(\frac{\partial \mathbf{W}}{\partial \mu} \frac{\partial \mathbf{U}}{\partial \lambda} + \frac{\partial \mathbf{W}}{\partial \lambda} \frac{\partial \mathbf{U}}{\partial \mu} \right) + tr \mathbf{U} \\
& \tilde{\mathbf{P}} \left(\frac{\partial \mathbf{U}^\dagger}{\partial \lambda} \frac{\partial \mathbf{W}}{\partial \mu} + \frac{\partial \mathbf{U}^\dagger}{\partial \mu} \frac{\partial \mathbf{W}}{\partial \lambda} \right)
\end{aligned} \quad (28)$$

$$\begin{aligned}
& - tr \tilde{\mathbf{P}} \frac{\partial \mathbf{U}^\dagger}{\partial \mu} (\mathbf{T} - \mathbf{W}) \frac{\partial \mathbf{U}}{\partial \lambda} - tr \tilde{\mathbf{P}} \frac{\partial \mathbf{U}^\dagger}{\partial \lambda} (\mathbf{T} - \mathbf{W}) \frac{\partial \mathbf{U}}{\partial \mu}
\end{aligned} \quad (29)$$

All terms in eqs 25–29 have been programmed (for the calculation of the derivatives of \mathbf{G} and \mathbf{U} , see Appendices A and B). Benchmark calculations reveal however that, for frequency calculations, all terms in eqs 26–29 can be neglected without leading to any significant errors (see below). This can be explained by considering that $\mathbf{U} = \mathbf{I} + O(c^{-2})$ for basis functions in the valence region,^{3,5} which holds also for the derivatives of the \mathbf{W} matrix. Also, the difference $\mathbf{I} - \mathbf{U}$ is on the order of $O(c^{-2})$. Thus, all terms in eqs 26–29 are on the order of $O(c^{-4})$. This is in line with the observations made in the case of the frequency calculations. Hence, the important terms of the second and second to last terms in eq 21 are given by eq 30

$$\begin{aligned}
& tr \frac{\partial \mathbf{P}}{\partial \mu} \frac{\partial \mathbf{H}_{1-e}}{\partial \lambda} + tr \mathbf{P} \frac{\partial^2 \mathbf{H}_{1-e}}{\partial \mu \partial \lambda} \\
& = tr(\mathbf{U} \tilde{\mathbf{P}} + \tilde{\mathbf{P}} \mathbf{U}^\dagger - \mathbf{U} \tilde{\mathbf{P}} \mathbf{U}^\dagger) \frac{\partial^2 \mathbf{T}}{\partial \mu \partial \lambda} + tr(\mathbf{U} \tilde{\mathbf{P}} \mathbf{U}^\dagger) \frac{\partial^2 \mathbf{W}}{\partial \mu \partial \lambda} \\
& + tr \tilde{\mathbf{P}} \frac{\partial^2 \mathbf{V}}{\partial \mu \partial \lambda} + tr \frac{\partial \mathbf{P}}{\partial \mu} \left(\frac{\partial \tilde{\mathbf{L}}}{\partial \lambda} \mathbf{G} + \mathbf{G}^\dagger \tilde{\mathbf{L}} \frac{\partial \mathbf{G}}{\partial \lambda} + \mathbf{G}^\dagger \frac{\partial \tilde{\mathbf{L}}}{\partial \lambda} \mathbf{G} \right) \\
& + tr \left(\mathbf{D} \frac{\partial^2 \mathbf{G}^\dagger}{\partial \mu \partial \lambda} + \mathbf{D}^\dagger \frac{\partial^2 \mathbf{G}}{\partial \mu \partial \lambda} \right) + tr \mathbf{P} \\
& \left[\left(\frac{\partial \mathbf{G}^\dagger}{\partial \mu} \frac{\partial \tilde{\mathbf{L}}}{\partial \lambda} + \frac{\partial \mathbf{G}^\dagger}{\partial \lambda} \frac{\partial \tilde{\mathbf{L}}}{\partial \mu} \right) \mathbf{G} + \mathbf{G}^\dagger \left(\frac{\partial \tilde{\mathbf{L}}}{\partial \lambda} \frac{\partial \mathbf{G}}{\partial \mu} + \frac{\partial \tilde{\mathbf{L}}}{\partial \mu} \frac{\partial \mathbf{G}}{\partial \lambda} \right) \right]
\end{aligned} \quad (30)$$

For the purpose of testing these simplifications and the individual contributions to eq 30 under different conditions, we calculated a set of three molecules listed in Table 1. Before analyzing the results in detail, a comment on the use of the finite nucleus model in the derivative calculations is appropriate. According to the data obtained, the differences caused by the use of a point charge or a finite nucleus model in connection with the $\partial^2 \mathbf{V} / \partial \mu \partial \lambda$ and $\partial^2 \mathbf{W} / \partial \mu \partial \lambda$ derivatives are negligible. The same is also true when calculating the energy gradient with regard to nuclear coordinates.³⁰ Accordingly, the finite nucleus model is used in connection with the corresponding molecular integrals when calculating single point energies. For the calculation of the first and second

derivatives of these integrals with respect to nuclear displacements, the point charge nuclear model is sufficient.

The dominant contributions in eq 30 result from the first four terms on the rhs. In term 4, the contributions from $\partial\mathbf{G}/\partial\lambda$ are much smaller than those from $\partial\tilde{\mathbf{L}}/\partial\lambda$. Our test calculations reveal that the contributions from terms 5 and 6 usually amount to less than 5 cm^{-1} in the frequencies. Whenever the accurate calculation of the Hessian matrix is not needed (for example, optimization of transition states or reaction path following), terms 5 and 6 can be neglected and term 4 approximated, thus significantly saving computer time and core memory. Derivative $\partial\tilde{\mathbf{L}}/\partial\lambda$ in term 6 can be replaced by $\partial\mathbf{V}/\partial\lambda$ (see discussion above), which also does not lead to any significant error (see Table 1).

Thus, the NESC Hessian (eq 21) comprises (i) the terms in eq 30 combined with the derivatives of the two-electron integrals and the overlap integrals obtained by using the usual nonrelativistic formalism, (ii) the derivatives $\partial\mathbf{P}/\partial\lambda$ of the density matrix, and (iii) the derivatives $\partial\mathbf{\Omega}/\partial\lambda$ of the molecular Lagrangian obtained using the NESC CP formalism described in Appendix C.

5. COMPUTATIONAL METHOD

The NESC contributions (eq 30) to the energy Hessian (eq 21) were programmed within the COLOGNE2011 program package³⁶ in connection with the analytic second derivative methodology of DFT³⁷ and MP2.³⁸ Special care was taken to obtain reliable first and second derivatives of matrices \mathbf{U} and \mathbf{G} . For this purpose, the problem of finding the first and second derivatives of \mathbf{G} was formulated in the form of a Sylvester equation, which was solved exactly using either the r-Smith or the eigenvalue decomposition method as described in Appendix A. For the exact calculation of $\partial\mathbf{U}/\partial\lambda$, response theory was employed (see Appendix B).³¹ Because the use of response theory for obtaining $\partial\mathbf{U}/\partial\lambda$ requires knowledge of the negative-energy (positronic) states, the one-step method⁷ for obtaining the matrix \mathbf{U} was used throughout this work.

In density functional calculations, two hybrid functionals were applied in this paper: PBE0³⁹ and B3LYP.⁴⁰ The ultrafine integration grid was used in the DFT calculations. In the MP2⁴¹ calculations, the 5d5f6s6p6d7s electrons of U and the 5f6s6p6d7s electrons of Cn were correlated.

The test calculations were carried out with a variety of all-electron basis sets^{42–48} (see Table 2), which in some cases had to be recontracted with a finite nucleus model possessing a Gaussian charge distribution.⁴⁹ Comparisons with relativistic effective core potentials (RECPs)⁴² were made throughout this work. For the velocity of light, the value $c = 137.035999070(98)\text{ a.u.}$ ⁵⁰ was used through the article.

Table 2. Specification of the Basis Sets Used in This Work

element	description	reference
H, C, O, F, S, Cl	hexathiocrownether-HgCl ₂ : recontracted 6-311G basis with a finite nucleus model	42
	in other calculations: recontracted def2-QZVPP with a finite nucleus model	42
Au, Hg, Tl	recontracted SARC with a finite nucleus model	43
U, No	DK3-Gen-Tk/NOSeC-VTZP	44, 45
No	SCF-DK3 with point charge nucleus model, uncontracted	46, 47
Cn (E112)	Dyall's triple- ζ basis set (32s29p20d13f), uncontracted	48

All NESC calculations were performed using the *diagonalize-then-contract* strategy.⁷ That is, the NESC equations were solved in the basis set of primitive functions, and after finishing the one-electron part, the resulting matrices were converted to the contracted basis set.³⁰ The calculation of the gradient and the Hessian of the one-electron part was also carried out in the set of primitive basis functions, which implied back and forth transformations, because the coupled perturbed parts had to be done in the basis of the contracted functions. Geometry optimizations were carried out with tight convergence criteria.

6. RESULTS AND DISCUSSION

In Table 3, NESC/PBE0 and NESC/MP2 geometries, vibrational frequencies, and zero-point energies (ZPE) of some di-, tri-, and penta-atomic molecules containing gold (Au, $Z = 79$), mercury (Hg, $Z = 80$), uranium (U, $Z = 92$), and copernicium (Cn, $Z = 112$) are listed and compared with experimental data and the results of some other high level calculations. The results of RECP calculations are also included in Table 3 for reasons of comparison with NESC results. For the purpose of demonstrating the influence of relativistic effects on calculated vibrational frequencies, vibrational frequencies without scalar relativistic corrections are given for the mercury hydrides and halides. As a proof for the general applicability of the NESC second derivative formalism, we have also calculated infrared intensities for all molecular vibrations (see Table 3). However, presentation and discussion of the formulas for obtaining these second order response properties is beyond the scope of this paper and will be presented elsewhere.

NESC/PBE0 frequencies deviate on average by just 5 cm^{-1} from the corresponding RECP values. However in those cases where the potential is steep in the quadratic range and the RECP geometry differs from the NESC geometry, differences between NESC and RECP vibrational frequencies can become larger (see, e.g., HgH and HgH₂ in Table 3). Changes in the vibrational frequencies due to relativistic effects range from -73 to 350 cm^{-1} and are on average 105 cm^{-1} . For the three diatomic molecules in Table 1, the vibrational frequency changes by 30% and more. For the infrared intensities, the differences are more distinct: The relativistic effects lead to changes by -133.6 up to 88.1 km/mol (standard deviation 52.2 km/mol), whereas the differences between NESC and RECP intensities range from -11.7 to 16.9 km/mol (standard deviation: 5.8 km/mol ; see Table 3).

NESC/PBE0 frequencies are close to experimental results where in some cases they are slightly larger in other cases somewhat smaller. Especially encouraging is the (Hg,Hg) stretching frequency of 21.2 cm^{-1} for the mercury dimer, which differs by just 2 cm^{-1} from the experimental value of 19.4 cm^{-1} .⁵¹ Similarly convincing results are obtained for the gold dimer (179 vs 191 cm^{-1})⁵² and the mercury–gold cation (152 vs 156 cm^{-1} ;⁵³ Table 3). The NESC/PBE0 description of the copernicium dimer (period 7 homologue of Hg, atomic number 112, longest half-lifetime measured: 28.5 s for isotope 285^{54}) leading to a interaction distance of 3.70 Å and a stretching frequency of 17 cm^{-1} is consistent with that for the mercury dimer. The NESC/MP2 results and the DKS/BP results of Schwerdtfeger and co-workers⁵⁵ for Cn₂ are similar.

In those cases where comparison with experimental results is not possible, close agreement with other high level methods is obtained as, e.g., with CCSD(T)/RECP calculations. This is the case for HgF₂, HgF₄, HgCl₂, HgCl₄, and to some extent also UO₂²⁺. It seems that the more reliable account of electron

Table 3. Comparison of NESC Geometries (Distances in Å), ZPE Values (kcal/mol), Vibrational Frequencies (cm^{-1}), and Infrared Intensities (km/mol) with the Corresponding Experimental and Other Quantum Chemical Values^a

mol.(symm.)	method	structure	ZPE	frequency, infrared intensity, and mode
HgH ($C_{\infty v}$)	NESC/PBE0	Hg–H: 1.747	1.93	1349.0 (103.4; σ^+)
	RECP/PBE0	Hg–H: 1.762	1.90	1327.1 (101.7; σ^+)
	NR/PBE0	Hg–H: 1.856	2.03	1421.9 (216.9; σ^+)
	exptl. ⁶⁹	Hg–H: 1.741	1.98	1385 (σ^+)
HgH ₂ ($D_{\infty h}$)	NESC/PBE0	Hg–H: 1.639	8.11	816.1 (33.3; π_u), 1964.4 (415.2; σ_u^+), 2077.1 (0; σ_g^+)
	RECP/PBE0	Hg–H: 1.646	8.10	808.0 (34.1; π_u), 1963.2 (426.9; σ_u^+), 2085.6 (0; σ_g^+)
	NR/PBE0	Hg–H: 1.768	6.64	592.9 (166.9; π_u), 1732.1 (371.7; σ_u^+), 1727.1 (0; σ_g^+)
	exptl. ⁷⁰	Hg–H: 1.633	8.07	770 (π_u), 1994.6 (σ_u^+), 2112 (σ_g^+)
HgH ₄ (D_{4h})	NESC/PBE0	Hg–H: 1.625	17.67	758.1 (0; b_{2g}), 771.2 (45.0; e_u), 856.8 (9.6; a_{2u}), 909.1 (0; b_{2u}), 2013.2 (346.3; e_u), 2123.0 (0; a_{1g}), 2145.8 (0; b_{1g})
	RECP/PBE0	Hg–H: 1.631	17.54	750.8 (0; b_{2g}), 762.8 (44.2; e_u), 848.6 (9.8; a_{2u}), 901.6 (0; b_{2u}), 1996.1 (354.3; e_u), 2111.5 (0; a_{1g}), 2138.6 (0; b_{1g})
	NR/PBE0	Hg–H: 1.728	14.83	563.6 (0; b_{2g}), 559.3 (49.8; e_u), 664.9 (70.1; a_{2u}), 771.9 (0; b_{2u}), 1808.9 (258.2; e_u), 1787.3 (0; a_{1g}), 1848.7 (0; b_{1g})
	MP2/RECP ⁷¹	Hg–H: 1.618	17.87	772 (0; b_{2g}), 757 (58; e_u), 842 (7; a_{2u}), 909 (0; b_{2u}), 2058 (310; e_u), 2154 (0; a_{1g}), 2194 (0; b_{1g})
HgF ($C_{\infty v}$)	NESC/PBE0	Hg–F: 2.039	0.64	444.9 (42.0; σ^+)
	RECP/PBE0	Hg–F: 2.047	0.64	446.2 (36.6; σ^+)
	NR/PBE0	Hg–F: 2.089	0.69	482.1 (74.5; σ^+)
	exptl. ⁷²		0.70	490.8 (σ^+)
HgF ₂ ($D_{\infty h}$)	NESC/PBE0	Hg–F: 1.910	2.31	179.6 (18.5; π_u), 590.3 (0; σ_g^+), 665.1 (126.7; σ_u^+)
	RECP/PBE0	Hg–F: 1.917	2.28	173.6 (15.2; π_u), 585.0 (0; σ_g^+), 660.4 (116.8; σ_u^+)
	NR/PBE0	Hg–F: 2.023	1.90	116.6 (32.9; π_u), 516.2 (0; σ_g^+), 580.1 (108.5; σ_u^+)
	CCSD(T)/RECP ⁷³	Hg–F: 1.914	2.31	180.1 (π_u), 590.3 (σ_g^+), 666.0 (σ_u^+)
HgF ₄ (D_{4h})	NESC/PBE0	Hg–F: 1.883	5.36	176.3 (0; b_{2u}), 227.5 (0; b_{2g}), 229.0 (22.7; a_{2u}), 253.9 (3.3; e_u), 607.5 (0; b_{1g}), 613.3 (0; a_{1g}), 691.7 (102.6; e_u)
	RECP/PBE0	Hg–F: 1.888	5.30	171.6 (0; b_{2u}), 224.6 (0; b_{2g}), 224.4 (17.7; a_{2u}), 251.4 (2.1; e_u), 604.0 (0; b_{1g}), 606.2 (0; a_{1g}), 687.3 (91.9; e_u)
	NR/PBE0	Hg–F: 1.960	4.63	133.2 (0; b_{2u}), 202.0 (0; b_{2g}), 186.5 (26.3; a_{2u}), 210.7 (2.2; e_u), 533.8 (0; b_{1g}), 521.2 (0; a_{1g}), 621.3 (64.0; e_u)
	CCSD(T)/RECP ⁷³	Hg–F: 1.889	5.26	180.1 (b_{2u}), 218.0 (b_{2g}), 225.8 (a_{2u}), 247.6 (e_u), 590.7 (b_{1g}), 597.9 (a_{1g}), 687.6 (e_u)
HgCl ($C_{\infty v}$)	NESC/PBE0	Hg–Cl: 2.389	0.39	273.2 (19.0; σ^+)
	RECP/PBE0	Hg–Cl: 2.403	0.39	270.2 (15.2; σ^+)
	NR/PBE0	Hg–Cl: 2.459	0.42	291.8 (37.1; σ^+)
	exptl. ⁷⁴	Hg–Cl: 2.395	0.42	293.4 (σ^+)
HgCl ₂ ($D_{\infty h}$)	NESC/PBE0	Hg–Cl: 2.249	1.40	103.1 (6.7; π_u), 359.0 (0; σ_g^+), 412.2 (62.6; σ_u^+)
	RECP/PBE0	Hg–Cl: 2.255	1.35	95.5 (4.6; π_u), 351.2 (0; σ_g^+), 403.6 (55.6; σ_u^+)
	NR/PBE0	Hg–Cl: 2.372	1.19	73.0 (11.7; π_u), 316.6 (0; σ_g^+), 371.7 (55.8; σ_u^+)
	CCSD(T)/RECP ⁷³	Hg–Cl: 2.258	1.40	102.2 (π_u), 360.5 (σ_g^+), 414.6 (σ_u^+)
HgCl ₄ (D_{4h})	NESC/PBE0	Hg–Cl: 2.295	2.94	71.9 (0; b_{2u}), 128.6 (4.5; a_{2u}), 145.8 (0; b_{2g}), 146.9 (0.1; e_u), 312.7 (0; b_{1g}), 337.2 (0; a_{1g}), 382.2 (36.7; e_u)
	RECP/PBE0	Hg–Cl: 2.300	2.89	69.6 (0; b_{2u}), 125.6 (2.3; a_{2u}), 142.1 (0; b_{2g}), 144.2 (0.6; e_u), 308.8 (0; b_{1g}), 331.8 (0; a_{1g}), 377.7 (30.7; e_u)
	NR/PBE0	Hg–Cl: 2.397	2.46	52.8 (0; b_{2u}), 101.1 (5.1; a_{2u}), 97.4 (0; b_{2g}), 112.4 (0.9; e_u), 277.1 (0; b_{1g}), 284.8 (0; a_{1g}), 342.5 (17.9; e_u)
	CCSD(T)/RECP ⁷³	Hg–Cl: 2.311	2.85	71.9 (b_{2u}), 123.0 (a_{2u}), 143.2 (b_{2g}), 142.6 (e_u), 293.7 (b_{1g}), 321.9 (a_{1g}), 379.1 (e_u)
Hg ₂ ($D_{\infty h}$)	NESC/PBE0	Hg–Hg: 3.587	0.03	21.2 (0; σ_g^+)
	RECP/PBE0	Hg–Hg: 3.663	0.02	14.6 (0; σ_g^+)
	exptl. ⁵¹	Hg–Hg: 3.629	0.03	19.4 (σ_g^+)
AuH ($C_{\infty v}$)	NESC/PBE0	Au–H: 1.530	3.26	2283.7 (14.7; σ^+)
	RECP/PBE0	Au–H: 1.534	3.25	2270.0 (15.0; σ^+)
	exptl. ⁷²	Au–H: 1.524	3.30	2305.0 (σ^+)
AuF ($C_{\infty v}$)	NESC/PBE0	Au–F: 1.923	0.80	556.7 (52.3; σ^+)
	RECP/PBE0	Au–F: 1.935	0.78	545.3 (47.2; σ^+)
	Exptl. ⁷⁵	Au–F: 1.918	0.81	563.7 (σ^+)
Au ₂ ($D_{\infty h}$)	NESC/PBE0	Au–Au: 2.506	0.26	179.0 (0; σ_g^+)

Table 3. continued

mol.(symm.)	method	structure	ZPE	frequency, infrared intensity, and mode
$\text{HgAu}^+ (C_{\infty v})$	RECP/PBE0	Au–Au: 2.511	0.25	176.5 (0; σ_g^+)
	exptl. ⁵²	Au–Au: 2.472	0.27	190.9 (σ_g^+)
	NESC/PBE0	Hg–Au: 2.563	0.22	152.0 (0.8; σ^+)
	RECP/PBE0	Hg–Au: 2.571	0.21	149.4 (0.9 σ^+)
	DC FSCC ⁵³	Hg–Au: 2.553	0.22	156 (σ^+)
$^{238}\text{UO}_2^{2+} (D_{\infty h})$	NESC/PBE0	U–O: 1.682	3.75	182.8 (21.1; π_u), 1087.7 (0; σ_g^+), 1171.4 (209.4; σ_u^+)
	RECP/PBE0	U–O: 1.676	3.76	183.3 (16.4; π_u), 1091.1 (0; σ_g^+), 1175.9 (192.5; σ_u^+)
	NESC/MP2	U–O: 1.712	3.29	138.0 (14.6; π_u), 961.3 (0; σ_g^+), 1066.8 (88.8; σ_u^+)
	CCSD(T)/RECP ⁷⁶	U–O: 1.690	3.59	178.4 (π_u), 1035.3 (σ_g^+), 1120.0 (σ_u^+)
$\text{C}^{238}\text{UO} (C_{\infty v})$	NESC/PBE0	U–C: 1.734, U–O: 1.779	3.26	95.0 (116.3; π), 916.3 (253.1; σ^+), 1174.7 (200.0; σ^+)
	RECP/PBE0	U–C: 1.730, U–O: 1.773	3.25	90.3 (106.5; π), 918.7 (244.2; σ^+), 1174.1 (192.0; σ^+)
	exptl. ⁷⁷			872.2 (σ^+), 1047.3 (σ^+)
	NESC/PBE0	Cn–Cn: 3.700	0.02	16.9 (0; σ_g^+)
$^{285}\text{Cn}_2 (D_{\infty h})$	NESC/MP2	Cn–Cn: 3.407	0.05	33.8 (0; σ_g^+)
	BP/DKS ⁵⁵	Cn–Cn: 3.45	0.04	25 (σ_g^+)

^aRECP calculation: ECP60MWB-SEG for U^{78} and def2-QZVPP for other atoms.⁴² For the nonrelativistic calculations (NR), the same basis set as in the NESC calculations was used. Intensities of π , π_u , and e_u modes have to be multiplied by the degeneracy factor $g = 2$.

correlation provided by CCSD(T) will be balanced by the more accurate relativistic description (NESC compared to the use of RECPs), if the latter is combined with the PBE0 functional. NESC/MP2 however seems to provide somewhat inferior results. The results for UO_2^{2+} reveal the typical tendency of MP2 to exaggerate pair-electron correlation and to lead to an artificial lengthening of bonds and thereby an underestimation of experimental frequencies.⁵⁶ It is noteworthy that, in all cases considered, ZPE values obtained with different computational approaches or based on experimental frequencies do not differ significantly, which is not unexpected in view of a conversion factor of 1/349.757 from cm^{-1} to kcal/mol.

Mercury in the oxidation state IV was realized by the synthesis and identification of HgF_4 in the matrix by Andrews and co-workers,⁵⁷ who pointed out that the existence of a Hg(IV) derivative suggested a $\text{Xe}4f^{14}5d^8$ electron configuration, the involvement of d electrons in bonding, and accordingly the chemical behavior typical of a transition metal. The NESC/PBE0 frequencies of HgH_n , HgF_n , and HgCl_n ($n = 1, 2, 4$) listed in Table 3 show some trends, which become clearer when calculated normal vibrational modes are converted into local vibrational modes.^{58–60} The NESC/PBE0 local mode vibrational force constants are given in Table 4. The local Hg-X ($X = \text{H, F, Cl}$) stretching force constants reflect the strength of the corresponding HgX bonds. They show that there is a small, but significant, increase in bond strength when HgF_4 is formed, which despite (F,F) repulsion leads to a stable tetrafluoride. In the case of the hydride, the increase in the strength of the HgH bond from the di- to the tetrahydride is small, whereas in the case of the chloride it is even reversed. We conclude that electronegativity of the ligand and the (ligand,ligand) repulsion are decisive for the formation of a stable Hg(IV) molecule.

NESC/PBE0 frequency calculations included calculations with 620 basis functions (e.g., Cn_2). For the purpose of calculating a system of direct chemical relevance, we calculated

Table 4. NESC/PBE0 Local Mode Force Constants k_a of Some Selected Hg- and U-Containing Molecules^a

mol (sym)	Hg–X [Å]	local mode force constant k_a [mdyn/Å]
$\text{HgH} (C_{\infty v})$	1.747	Hg–H: 1.075
$\text{HgH}_2 (D_{\infty h})$	1.639	Hg–H: 2.406; H–Hg–H: 0.148
$\text{HgH}_4 (D_{4h})$	1.625	Hg–H: 2.486; H–Hg–H: 0.124; out-of-plane: 0.665
$\text{HgF} (C_{\infty v})$	2.039	Hg–F: 2.025
$\text{HgF}_2 (D_{\infty h})$	1.910	Hg–F: 3.969; F–Hg–F: 0.155
$\text{HgF}_4 (D_{4h})$	1.883	Hg–F: 4.320; F–Hg–F: 0.300; out-of-plane: 0.764
$\text{HgCl} (C_{\infty v})$	2.389	Hg–Cl: 1.311
$\text{HgCl}_2 (D_{\infty h})$	2.249	Hg–Cl: 2.628; Cl–Hg–Cl: 0.116
$\text{HgCl}_4 (D_{4h})$	2.295	Hg–Cl: 2.199; Cl–Hg–Cl: 0.287; out-of-plane: 0.413
$^{238}\text{UO}_2^{2+} (D_{\infty h})$	1.712	U–O: 11.273; O–U–O: 0.108
$\text{C}^{238}\text{UO} (C_{\infty v})$	1.734, 1.779	U–C: 9.264; U–O: 7.456; C–U–O: 0.028

^aStretching force constants in mdyn/Å, bending force constants in $\text{mdyn} \cdot \text{Å}/\text{rad}^2$.

the mercury crownthioether shown in Figure 1, which has been discussed in connection with the removal of mercury from the environment.⁶¹ Although the primitive and contracted basis set involved 998 and 597 basis functions in this case, the calculation of the vibrational frequencies turned out to require only slightly more than the time of a nonrelativistic frequency calculations depending however on the accuracy required. Since the interactions of the Hg atom with the six S atoms are relatively weak, we expected that only some frequencies in the low range are affected by the relativistic corrections and that RECP calculations with the XC functional and basis similar to those used in the NESC calculations should lead to similar frequencies. Hence, we used the mercury(II)chloride hexathia-crown complex of Figure 1 as a test case for the reliability and

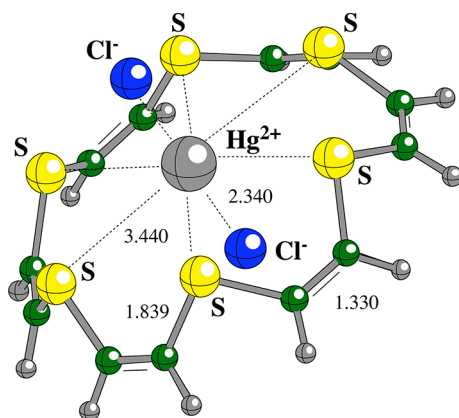


Figure 1. NESC/B3LYP geometry of the C_{6v} -symmetrical Hg(II)Cl_2 hexathia-18-crown-6 complex (distances in Å).

feasibility of NESC second derivative calculations in the case of larger molecules. The results listed in Table 5 show that

Table 5. Vibrational Frequencies (cm^{-1}) of the HgCl_2 Hexathia-18-crown-6 Complex (C_{6v}) Obtained at the NESC/B3LYP and RECP/B3LYP Levels of Theory (ZPE: 129.03 kcal/mol)

mode	method	frequency [cm^{-1}]
a_1	NESC	36.3, 131.3, 177.4, 291.6, 350.5, 624.8, 734.3, 1223.2, 1650.2, 3187.9
	RECP	36.2, 131.4, 176.4, 294.1, 353.2, 624.9, 734.7, 1226.4, 1647.6, 3185.3
a_2	NESC	383.4, 533.3, 722.0, 931.5, 1293.8, 3161.9
	RECP	384.2, 535.1, 723.1, 932.3, 1297.0, 3158.1
b_1	NESC	53.3, 162.4, 618.0, 679.7, 1201.9, 1607.5, 3189.2
	RECP	55.0, 163.3, 618.8, 680.5, 1204.7, 1604.8, 3185.4
b_2	NESC	62.3, 137.7, 457.2, 514.6, 828.2, 948.8, 1347.9, 3160.9
	RECP	62.7, 139.1, 457.1, 515.0, 828.7, 949.3, 1352.0, 3158.0
e_1	NESC	45.1, 53.7, 90.6, 122.9, 200.4, 400.8, 514.7, 629.1, 716.6, 762.6, 936.8, 1216.3, 1315.1, 1638.9, 3161.7, 3188.1
	RECP	42.2, 50.0, 87.5, 123.1, 200.3, 401.2, 516.1, 629.7, 717.3, 763.4, 937.5, 1219.4, 1318.5, 1636.4, 3158.5, 3184.0
e_2	NESC	31.8, 56.0, 116.2, 197.7, 443.0, 501.4, 626.4, 692.8, 809.4, 945.0, 1205.9, 1338.9, 1617.9, 3161.1, 3188.9
	RECP	33.3, 56.4, 116.5, 198.7, 442.7, 502.3, 627.3, 693.5, 810.0, 945.5, 1208.8, 1342.7, 1615.3, 3157.4, 3184.8

NESC/B3LYP/SARC/6-311G and B3LYP/RECP/6-311G calculations lead to the same ZPE value and similar frequencies, which differ only by 3 to 4 cm^{-1} in the low-frequency range. Hence, the NESC second derivative program developed in this work is reliable also in the case of large molecule calculations.

7. CONCLUSIONS

In this work, we have extended the applicability spectrum of the NESC method, which provides an exact two-component relativistic description for molecules with heavy and superheavy atoms.

1. We have developed the methodology for routinely calculating second order response properties with the help of analytic second energy derivatives for the NESC method within its scalar relativistic form.
2. We have outlined and programmed a computationally efficient algorithm to calculate the NESC Hessian also in the presence of basis functions with very large exponents (*steep basis functions*). A versatile, generally applicable

algorithm is a prerequisite for NESC calculations in combination with HF, DFT, or correlation corrected ab initio calculations such as CI, MPn perturbation theory, coupled cluster theory, CASSCF, or any other non-relativistic method provided that analytic second derivatives are available for the latter methods.

3. Special care has been laid on the calculation of first and second derivatives of the renormalization matrix \mathbf{G} (i.e., considering the so-called *picture change*) and the matrix representation of the operator \hat{U} for the elimination of the small component. For this purpose, this problem was cast in the form of a Sylvester equation, for which the exact solution was worked out. Also, the determination of $\partial\mathbf{U}/\partial\lambda$ via response theory recently described³¹ has been extended to the corresponding second derivatives.
4. The development of the NESC Hessian was done considering a finite nucleus model and the correct *picture change*, i.e., renormalization of the NESC Hamiltonian.
5. The economic implementation of the analytic NESC energy Hessian and its general applicability is emphasized by presenting NESC/DFT vibrational frequency calculations with 1000 primitive basis functions for organic mercury compounds. Benchmark calculations testing the accuracy of the algorithm developed were carried out with 1500 basis functions.
6. NESC/PBE0 vibrational frequencies are in reasonable agreement with available experimental values and the results of other high level quantum chemical calculations.
7. In the cases of the mercury and the copernicium dimer, accurate stretching frequencies of 21 and 17 cm^{-1} have been obtained using the relativistic corrections obtained with NESC.
8. By converting calculated NESC/DFT vibrational modes into local vibrational modes and determining local stretching force constants, we have made predictions for the formation of Hg(IV) molecules.
9. In all cases considered, the CPU time needed for the calculation of the NESC vibrational frequencies is less than 5% larger than that needed for the corresponding calculation of nonrelativistic vibrational frequencies carried out with the same ab initio or DFT method and the same basis set.

In summary, we have proven that analytic NESC second derivative calculations can routinely be carried out and that in this way NESC second order response properties become available. The applicability range and the usefulness of NESC have been substantially increased. The methodology presented in this work is also of relevance for other exact two-component relativistic methods such as IOTC or X2C.

A. APPENDIX: THE FIRST AND SECOND DERIVATIVES OF THE RENORMALIZATION MATRIX \mathbf{G}

By differentiating eq 12 once or twice, one obtains a special case of the Sylvester equation:

$$\mathbf{GX} + \mathbf{XG} = \mathbf{Q} \quad (\text{A1})$$

with

$$\mathbf{Q} = \tilde{\mathbf{S}}^{-1} \left(\frac{\partial \mathbf{S}}{\partial \lambda} - \frac{\partial \tilde{\mathbf{S}}}{\partial \lambda} \mathbf{G} \mathbf{G} \right) \quad (\text{A2})$$

for $\mathbf{X} = \partial \mathbf{G} / \partial \lambda$ and

$$\mathbf{Q} = \tilde{\mathbf{S}}^{-1} \left[\frac{\partial^2 \mathbf{S}}{\partial \mu \partial \lambda} - \frac{\partial^2 \tilde{\mathbf{S}}}{\partial \mu \partial \lambda} \mathbf{G} \mathbf{G} + \frac{\partial \tilde{\mathbf{S}}}{\partial \lambda} \tilde{\mathbf{S}}^{-1} \left(\frac{\partial \tilde{\mathbf{S}}}{\partial \mu} \mathbf{G} \mathbf{G} - \frac{\partial \mathbf{S}}{\partial \mu} \right) + \frac{\partial \tilde{\mathbf{S}}}{\partial \mu} \tilde{\mathbf{S}}^{-1} \left(\frac{\partial \tilde{\mathbf{S}}}{\partial \lambda} \mathbf{G} \mathbf{G} - \frac{\partial \mathbf{S}}{\partial \lambda} \right) \right] - \frac{\partial \mathbf{G}}{\partial \lambda} \frac{\partial \mathbf{G}}{\partial \mu} - \frac{\partial \mathbf{G}}{\partial \mu} \frac{\partial \mathbf{G}}{\partial \lambda} \quad (\text{A3})$$

for $\mathbf{X} = \partial^2 \mathbf{G} / \partial \mu \partial \lambda$.

Here, we prove that the renormalization matrix given in eq 11 is positive definite. The matrices \mathbf{S} and \mathbf{T} are both positive definite (provided the basis set does not contain any linear dependencies). Johnson proved that $\mathbf{A} = \mathbf{B}^\dagger \mathbf{B}$ is positive definite only if \mathbf{B} is invertible.⁶² Hence, both $\tilde{\mathbf{S}}$ and $\mathbf{S}^{-1/2} \tilde{\mathbf{S}} \mathbf{S}^{-1/2}$ are positive definite, and their square-root matrices exist. Since always positive eigenvalues are taken in the calculation of the square-root matrix, $\mathbf{K} = (\mathbf{S}^{-1/2} \tilde{\mathbf{S}} \mathbf{S}^{-1/2})^{-1/2}$ is also positive definite. Then, \mathbf{G} is also positive definite because both \mathbf{G} and \mathbf{K} are similar matrices. If the eigenvectors of \mathbf{K} are collected in matrix \mathbf{R}_K (\mathbf{R}_K is a real matrix because of the hermitian nature of \mathbf{K}), then one can obtain the eigenvectors of \mathbf{G} from $\mathbf{R}_G = \mathbf{S}^{-1/2} \mathbf{R}_K$, which are also real. For a positive definite renormalization matrix \mathbf{G} with real eigenvectors as given by eq 11, the Sylvester equation can always be solved, i.e., the existence of the real solution \mathbf{X} is guaranteed. As we will show in the following, there are no special requirements with regard to matrix \mathbf{R}_G , which, for example, can be nonhermitian.

As contributions from the first derivative of \mathbf{G} are on the order of 10^{-4} or less, the last two terms in eq A3 can be neglected. The contributions from the first and second derivatives of \mathbf{U} are on the order of $O(c^{-4})$ in view of the prefactor of $1/2mc^2$ of the second term in eq 4. Therefore, one can simplify the derivatives of $\tilde{\mathbf{S}}$ as follows:

$$\frac{\partial \tilde{\mathbf{S}}}{\partial \lambda} \approx \frac{\partial \mathbf{S}}{\partial \lambda} + \frac{1}{2mc^2} \mathbf{U}^\dagger \frac{\partial \mathbf{T}}{\partial \lambda} \mathbf{U} \quad (\text{A4})$$

and

$$\frac{\partial^2 \tilde{\mathbf{S}}}{\partial \mu \partial \lambda} \approx \frac{\partial^2 \mathbf{S}}{\partial \mu \partial \lambda} + \frac{1}{2mc^2} \mathbf{U}^\dagger \frac{\partial^2 \mathbf{T}}{\partial \mu \partial \lambda} \mathbf{U} \quad (\text{A5})$$

In eqs A4 and A5, the first and second derivatives of \mathbf{S} (or \mathbf{T}) can be precalculated and saved in three ($\partial \mathbf{S} / \partial x$, $\partial \mathbf{S} / \partial y$, and $\partial \mathbf{S} / \partial z$) and six ($\partial^2 \mathbf{S} / \partial x \partial x$, $\partial^2 \mathbf{S} / \partial x \partial y$, $\partial^2 \mathbf{S} / \partial x \partial z$, $\partial^2 \mathbf{S} / \partial y \partial y$, $\partial^2 \mathbf{S} / \partial y \partial z$, and $\partial^2 \mathbf{S} / \partial z \partial z$) lower triangular matrices, respectively. In this work, two efficient methods for solving the Sylvester equation were programmed: (i) the r-Smith method and (ii) the eigenvalue decomposition method.

The r-Smith Iterative Method

The r-Smith method is based on an iterative procedure and requires that \mathbf{G} is positive definite, which is the case (see above). In the original Smith iterative method,⁶³ the general Sylvester equation

$$\mathbf{A} \mathbf{X} + \mathbf{X} \mathbf{B} = \mathbf{C} \quad (\text{A6})$$

is transformed into a Stein equation:

$$(\mathbf{A} + \mu \mathbf{I}) \mathbf{X} (\mathbf{B} + \mu \mathbf{I}) - (\mathbf{A} - \mu \mathbf{I}) \mathbf{X} (\mathbf{B} - \mu \mathbf{I}) = 2\mu \mathbf{C}$$

$$\mathbf{X} = 2\mu (\mathbf{A} + \mu \mathbf{I})^{-1} \mathbf{C} (\mathbf{B} + \mu \mathbf{I})^{-1} + [(\mathbf{A} + \mu \mathbf{I})^{-1} (\mathbf{A} - \mu \mathbf{I})] \mathbf{X} [(\mathbf{B} - \mu \mathbf{I}) (\mathbf{B} + \mu \mathbf{I})^{-1}] \quad (\text{A7})$$

which can be written as

$$\mathbf{X} = \mathbf{X}_0 + \Phi \mathbf{X} \Gamma \quad (\text{A8})$$

where $\mu \geq \text{Max}(A_{1,1}, A_{2,2}, \dots, A_{M,M}; B_{1,1}, B_{2,2}, \dots, B_{M,M})$ (M : number of basis functions) is a scalar constant,⁶⁴ and the generalized inverse matrix is defined by

$$\mathbf{M}^\dagger = (\mathbf{M}^\dagger \mathbf{M})^{-1} \mathbf{M}^\dagger = \mathbf{M}^\dagger (\mathbf{M} \mathbf{M}^\dagger)^{-1} \quad (\text{A9})$$

The iterative solution of eq A8 proceeds according to Smith⁶³ using eq A10

$$\mathbf{X}_{k+1} = \mathbf{X}_0 + \sum_{i=1}^k \Phi^i \mathbf{X}_0 \Gamma^i \quad (\text{A10})$$

There are several improved iterative Smith methods to accelerate convergence. Zhou and co-workers⁶⁵ replaced eq A10 by

$$\begin{cases} \mathbf{X}_{k+1} = \mathbf{X}_k + \sum_{i=1}^{r-1} \Phi_k^i \mathbf{X}_k \Gamma_k^i, & k \geq 0, r \geq 2, \\ \Phi_{k+1} = \Phi_k^r, & \Gamma_{k+1} = \Gamma_k^r, \\ \Phi_0 = \Phi, & \Gamma_0 = \Gamma, \end{cases} \quad (\text{A11})$$

which is the *r-Smith iterative method*. If \mathbf{A} and \mathbf{B} are not positive definite, $\rho(\Phi)\rho(\Gamma) > 1$ and the iterative procedure will diverge.

In the case of the first derivative of \mathbf{G} , the minimum number of matrix multiplications is about $9N[(r-1)(N_{\text{iter}}-1)+r]$ for $3N$ Sylvester equations (N : number of atoms in a molecule). The optimal μ value is given by $\text{Max}(\mathbf{G}_{ii})$.⁶⁴ In this case, the convergence ratio is $10^{-3} - 10^{-5}$; that is, if the maximum deviation between iterations $k-1$ and k is 10^{-8} , the accuracy of iteration k will be about 10^{-12} . Usually, $r=2$ and $N_{\text{iter}}=1-2$ if the accuracy of 10^{-12} is required. For this situation, the number of matrix multiplications is on the average $20N$. For geometry optimizations and frequency calculations as well as energy calculations using a finite nucleus model, the r-Smith method is the method of choice. However, for a few test calculations with a point nucleus model and steep basis functions (exponent larger than 10^{12}), the following algorithm turned out to be somewhat more costly (for $N_{\text{iter}}=1$ as in 80% of all calculations), but numerically more stable.

The Eigenvalue Decomposition Method

For the case of a hermitian matrix \mathbf{G} in eq 12, the eigenvalue decomposition method was previously used by several authors.^{29,66,67} In the following, this method will be extended to the case of a non-hermitian matrix \mathbf{G} .

Starting from the general Sylvester eq A6, let us diagonalize the non-hermitian matrices \mathbf{A} and \mathbf{B}

$$\mathbf{A} \mathbf{R}_A = \mathbf{R}_A \mathbf{E}_A \quad (\text{A12})$$

$$\mathbf{B} \mathbf{R}_B = \mathbf{R}_B \mathbf{E}_B \quad (\text{A13})$$

by multiplying them by their right eigenvectors \mathbf{R}_A and \mathbf{R}_B , respectively. Using the generalized inverse matrix A9, eqs A12 and A13 can be written as

$$\mathbf{E}_A = \mathbf{R}_A^\dagger \mathbf{A} \mathbf{R}_A \quad (\text{A14})$$

and

$$\mathbf{E}_B = \mathbf{R}_B^\dagger \mathbf{B} \mathbf{R}_B \quad (\text{A15})$$

respectively. Let us rewrite the Sylvester equation as in eq A16:

$$\mathbf{A} \mathbf{R}_A \mathbf{R}_A^\dagger \mathbf{X} + \mathbf{X} \mathbf{R}_B \mathbf{R}_B^\dagger \mathbf{B} = \mathbf{C} \quad (\text{A16})$$

Multiplying eq A16 by \mathbf{R}_A^\top from the left and by \mathbf{R}_B^\top from the right and using eqs A14 and A15, one obtains

$$\varepsilon_A \mathbf{R}_A^\top \mathbf{X} \mathbf{R}_B + \mathbf{R}_A^\top \mathbf{X} \mathbf{R}_B \varepsilon_B = \mathbf{R}_A^\top \mathbf{C} \mathbf{R}_B \quad (\text{A17})$$

or in a simpler form

$$\varepsilon_A \tilde{\mathbf{X}} + \tilde{\mathbf{X}} \varepsilon_B = \tilde{\mathbf{C}} \quad (\text{A18})$$

where a new matrix $\tilde{\mathbf{X}} = \mathbf{R}_A^\top \mathbf{X} \mathbf{R}_B$ is used. The elements of matrix $\tilde{\mathbf{X}}$ can be calculated using eq A19:

$$\tilde{X}_{i,j} = \frac{\tilde{C}_{i,j}}{\varepsilon_{A_i,i} + \varepsilon_{B_j,j}} \quad (\text{A19})$$

and matrix \mathbf{X} can be obtained by back transformation

$$\mathbf{X} = \mathbf{R}_A \tilde{\mathbf{X}} \mathbf{R}_B^\top \quad (\text{A20})$$

Since both eigenvalues and eigenvectors of \mathbf{G} are real (see above), there is no necessity for complex matrix algebra. About the same number of matrix multiplications as in the r-Smith method are needed; however, the diagonalizations slightly increase the cost compared to an r-Smith calculation with $r = 2$ (normal case).

For a benchmark calculation of the gradient with 33 atoms (solution of 99 Sylvester equations) and 1500 basis functions, both methods took about 10 minutes on a single processor. However, routine calculations of the NESC gradient are efficiently carried out in parallel.

B. APPENDIX: CALCULATION OF THE FIRST AND SECOND DERIVATIVES OF \mathbf{U} WITH THE HELP OF RESPONSE THEORY

Although the methods discussed so far can provide sufficient numeric accuracy for the geometry optimizations and vibrational frequency calculations with the NESC method, the calculation of some other first and second order response properties may require the determination of the exact first and second derivatives of the elimination of the small component operator \mathbf{U} . In these cases, the following approach is the method of choice.

Calculation of the First Derivatives of \mathbf{U}

Denoting the matrix operator on the left hand side of eq 1 as $\tilde{\mathbf{D}}$, the metric matrix on the right hand side as $\tilde{\mathbf{M}}$, the four-component wavefunction as Φ , and the matrix of the eigenvalues as ε ; differentiating eq 1 with respect to a perturbation λ ; and multiplying the resulting equation by Φ^\dagger from the left, one arrives at eq B1:

$$\mathbf{O}^\lambda \varepsilon - \varepsilon \mathbf{O}^\lambda + \varepsilon^\lambda = \Phi^\dagger \tilde{\mathbf{D}}^\lambda \Phi - \Phi^\dagger \tilde{\mathbf{M}}^\lambda \Phi \varepsilon \quad (\text{B1})$$

in which the relationships $\Phi^\dagger \tilde{\mathbf{D}} \Phi = \varepsilon$ and $\Phi^\dagger \tilde{\mathbf{M}} \Phi = \mathbf{I}$ were used, and ε^λ , $\tilde{\mathbf{D}}^\lambda$, and $\tilde{\mathbf{M}}^\lambda$ denote the derivatives of the corresponding matrices with respect to the parameter λ . In eq B1, an operator \mathbf{O}^λ is introduced, which connects the derivative of the four-component wavefunction with Φ as in eq B2

$$\Phi^\lambda = \Phi \mathbf{O}^\lambda \quad (\text{B2})$$

Operator \mathbf{O}^λ plays the central role for obtaining the derivatives $\partial \mathbf{U} / \partial \lambda$. Its matrix elements are given in eq B3.

$$O_{ij}^\lambda = \begin{cases} \frac{(\Phi^\dagger \tilde{\mathbf{D}}^\lambda \Phi)_{ij} - (\Phi^\dagger \tilde{\mathbf{M}}^\lambda \Phi)_{ij} \varepsilon_j}{\varepsilon_j - \varepsilon_i} & \text{for } i \neq j \\ -\frac{1}{2} (\Phi^\dagger \tilde{\mathbf{M}}^\lambda \Phi)_{ii} & \text{for } i = j \end{cases} \quad (\text{B3})$$

Note that the diagonal elements of \mathbf{O}^λ are obtained by differentiating the normalization condition of the four-component wavefunction Φ and that \mathbf{O}^λ is a non-symmetric matrix.

Next, eq B2 is rewritten in terms of individual components of the four-component wavefunction Φ .

$$\begin{pmatrix} \mathbf{A}_-^\lambda & \mathbf{A}_+^\lambda \\ \mathbf{B}_-^\lambda & \mathbf{B}_+^\lambda \end{pmatrix} = \begin{pmatrix} \mathbf{A}_- & \mathbf{A}_+ \\ \mathbf{B}_- & \mathbf{B}_+ \end{pmatrix} \begin{pmatrix} \mathbf{O}_1^\lambda & \mathbf{O}_2^\lambda \\ \mathbf{O}_3^\lambda & \mathbf{O}_4^\lambda \end{pmatrix} \\ = \begin{pmatrix} \mathbf{A}_- \mathbf{O}_1^\lambda + \mathbf{A}_+ \mathbf{O}_3^\lambda & \mathbf{A}_- \mathbf{O}_2^\lambda + \mathbf{A}_+ \mathbf{O}_4^\lambda \\ \mathbf{B}_- \mathbf{O}_1^\lambda + \mathbf{B}_+ \mathbf{O}_3^\lambda & \mathbf{B}_- \mathbf{O}_2^\lambda + \mathbf{B}_+ \mathbf{O}_4^\lambda \end{pmatrix} \quad (\text{B4})$$

As can be seen from eq B4, the response of the large and small components of the electronic states involves mixing with the positronic states via the negative-positive block \mathbf{O}_2^λ of the response operator \mathbf{O}^λ . Apparently, this is not the same as eq 33 of ref 28. In that paper, the contributions of the positronic wavefunction were neglected and only the last terms in \mathbf{A}_+^λ and \mathbf{B}_+^λ kept. In this connection, we note that the formalism proposed by Reiher and Wolf,⁶⁸ which is based on the exact decoupling of electronic and positronic states by a perturbation-independent transformation, should lead to the vanishing of the response operator \mathbf{O}_2^λ and consequently of the derivative $\partial \mathbf{U} / \partial \mathbf{U} d\lambda$.

By differentiating eq 3 with regard to λ and substituting eq B4, one obtains eq B5 for $\partial \mathbf{U} / \partial \lambda$.

$$\frac{\partial \mathbf{U}}{\partial \lambda} = \mathbf{U}^\lambda = (\mathbf{B}_- - \mathbf{U} \mathbf{A}_-) \mathbf{O}_2^\lambda \mathbf{A}_+^\dagger \tilde{\mathbf{S}} \quad (\text{B5})$$

In explicit form, the matrix elements \mathbf{O}_2^λ are given by eq B6:

$$(\mathbf{O}_2^\lambda)_{ij} = \frac{(\Phi^\dagger \tilde{\mathbf{D}}_2^\lambda \Phi)_{ij} - (\Phi^\dagger \tilde{\mathbf{M}}_2^\lambda \Phi)_{ij} (\varepsilon_+)_j}{(\varepsilon_+)_j - (\varepsilon_-)_i} \quad (\text{B6})$$

where index i runs over positronic states, index j over electronic states, and the following negative–positive blocks of the $\tilde{\mathbf{D}}$ and $\tilde{\mathbf{M}}$ matrices are introduced

$$\Phi^\dagger \tilde{\mathbf{D}}_2^\lambda \Phi = \mathbf{A}_-^\dagger \frac{\partial \mathbf{V}}{\partial \lambda} \mathbf{A}_+ + \mathbf{A}_-^\dagger \frac{\partial \mathbf{T}}{\partial \lambda} \mathbf{B}_+ + \mathbf{B}_-^\dagger \frac{\partial \mathbf{T}}{\partial \lambda} \mathbf{A}_+ \\ + \mathbf{B}_-^\dagger \left(\frac{\partial \mathbf{W}}{\partial \lambda} - \frac{\partial \mathbf{T}}{\partial \lambda} \right) \mathbf{B}_+ \quad (\text{B7})$$

$$\Phi^\dagger \tilde{\mathbf{M}}_2^\lambda \Phi = \mathbf{A}_-^\dagger \frac{\partial \mathbf{S}}{\partial \lambda} \mathbf{A}_+ + (2mc^2)^{-1} \mathbf{B}_-^\dagger \frac{\partial \mathbf{T}}{\partial \lambda} \mathbf{B}_+ \quad (\text{B8})$$

Equation 20 contains the contributions of the operator $\partial \mathbf{U} / \partial \lambda$ to the NESC energy derivative. These contributions are always given by traces of matrix products:

$$\text{tr} \mathbf{P}_0 \frac{\partial \mathbf{U}}{\partial \lambda} = \text{tr} \mathbf{A}_+^\dagger \tilde{\mathbf{S}} \mathbf{P}_0 (\mathbf{B}_- - \mathbf{U} \mathbf{A}_-) \mathbf{O}_2^\lambda = \text{tr} \mathbf{M}' \mathbf{O}_2^\lambda \quad (\text{B9})$$

where a new matrix $\mathbf{M}' = \mathbf{A}_+^\dagger \tilde{\mathbf{S}} \mathbf{P}_0 (\mathbf{B}_- - \mathbf{U} \mathbf{A}_-)$ is introduced. Because the elements of the operator \mathbf{O}_2^λ are expressed in terms of quadratic forms of the general type $\mathbf{C}_-^\dagger (\partial \mathbf{X} / \partial \lambda) \mathbf{C}_+$ where $\mathbf{C} =$

\mathbf{A} and \mathbf{B} and $\partial\mathbf{X}/\partial\lambda$ is a matrix of the derivatives of the molecular integrals, the trace in eq B9 can be transformed as in eq B12:

$$\begin{aligned} \text{tr} \mathbf{M}' & \left\{ \frac{1}{(\varepsilon_+)_j - (\varepsilon_-)_i} \left(\mathbf{C}_+^\dagger \frac{\partial \mathbf{Y}}{\partial \lambda} \mathbf{C}_+ \right)_{ij} \right\} \\ &= \sum_{i,j} \sum_{a,b} \frac{M'_{ji}}{(\varepsilon_+)_j - (\varepsilon_-)_i} (\mathbf{C}_-^\dagger)_{ia} \frac{\partial Y_{ab}}{\partial \lambda} (\mathbf{C}_+)_bj \end{aligned} \quad (\text{B10})$$

$$= \sum_{a,b} \left(\sum_{i,j} (\mathbf{C}_+)_bj \frac{M'_{ji}}{(\varepsilon_+)_j - (\varepsilon_-)_i} (\mathbf{C}_-^\dagger)_{ia} \right) \frac{\partial Y_{ab}}{\partial \lambda} \quad (\text{B11})$$

$$= \text{tr} \mathbf{Z} \frac{\partial \mathbf{Y}}{\partial \lambda} \quad (\text{B12})$$

where \mathbf{Z} is a matrix with the elements given by the term in parentheses in eq B11. Thus, the contributions of the \mathbf{U}^λ operator to the energy gradient can be conveniently formulated in terms of traces of matrix products. After some algebraic transformations, one arrives at eq B13 for the contribution of $\partial\mathbf{U}/\partial\lambda$

$$\text{tr} \left(\mathbf{P}_0^\dagger \frac{\partial \mathbf{U}^\dagger}{\partial \lambda} + \mathbf{P}_0 \frac{\partial \mathbf{U}}{\partial \lambda} \right) = \sum_{\mathbf{Y}=\mathbf{S},\mathbf{T},\mathbf{V},\mathbf{W}} \left[\text{tr} (\mathbf{P}_Y + \mathbf{P}_Y^\dagger) \frac{\partial \mathbf{Y}}{\partial \lambda} \right] \quad (\text{B13})$$

however, with the new matrices \mathbf{P}_Y ($\mathbf{Y} = \mathbf{S}, \mathbf{T}, \mathbf{V}, \mathbf{W}$) given in the following.

$$(\mathbf{P}_S)_{\nu\mu} = - \sum_{i,j} (\mathbf{A}_+)_\mu j (\mathbf{A}_-)_\nu i \frac{(\varepsilon_+)_j M'_{ji}}{(\varepsilon_+)_j - (\varepsilon_-)_i} \quad (\text{B14})$$

$$\begin{aligned} (\mathbf{P}_T)_{\nu\mu} &= \sum_{i,j} \left\{ (\mathbf{B}_+)_\mu j (\mathbf{A}_-)_\nu i + (\mathbf{A}_+)_\mu j (\mathbf{B}_-)_\nu i - \left(1 + \frac{\varepsilon_j^+}{2mc^2} \right) \right. \\ & \quad \left. (\mathbf{B}_+)_\mu j (\mathbf{B}_-)_\nu i \right\} \frac{M'_{ji}}{(\varepsilon_+)_j - (\varepsilon_-)_i} \end{aligned} \quad (\text{B15})$$

$$(\mathbf{P}_V)_{\nu\mu} = \sum_{i,j} (\mathbf{A}_+)_\mu j (\mathbf{A}_-)_\nu i \frac{M'_{ji}}{(\varepsilon_+)_j - (\varepsilon_-)_i} \quad (\text{B16})$$

$$(\mathbf{P}_W)_{\nu\mu} = \sum_{i,j} (\mathbf{B}_+)_\mu j (\mathbf{B}_-)_\nu i \frac{M'_{ji}}{(\varepsilon_+)_j - (\varepsilon_-)_i} \quad (\text{B17})$$

Thus, eq B13 together with eqs B14–B17 completes the derivation of the exact NESC analytic gradient. These equations can be used in connection with analytic gradient geometry optimizations or in connection with the first-order response formalism for obtaining various molecular properties. Since the calculation of the first derivative of \mathbf{U} does not cost much, it is always calculated in geometry optimizations unless steep basis functions are used as reflected by $\text{Max}(\varepsilon_+) > 10^6$ (for the definition of ε_+ , see eq 1).

Calculation of the Second Derivatives of \mathbf{U}

By introducing a new operator $\tilde{\mathbf{O}}^{\mu\lambda}$ via

$$\Phi^{\mu\lambda} = \Phi(\mathbf{O}^{\mu\lambda} + \mathbf{O}^\mu \mathbf{O}^\lambda) = \Phi \tilde{\mathbf{O}}^{\mu\lambda} \quad (\text{B18})$$

and differentiating eq B5 with respect to external parameters μ , one obtains for $\mathbf{U}^{\mu\lambda}$ the following equation

$$\begin{aligned} \mathbf{U}^{\mu\lambda} &= (\mathbf{B}_- - \mathbf{U}\mathbf{A}_-)(\tilde{\mathbf{O}}_2^{\mu\lambda} - \mathbf{O}_2^\mu \mathbf{O}_4^\lambda - \mathbf{O}_2^\lambda \mathbf{O}_4^\mu \\ & \quad - \mathbf{O}_2^\mu \mathbf{A}_+^\dagger \tilde{\mathbf{S}} \mathbf{A}_- \mathbf{O}_2^\lambda - \mathbf{O}_2^\lambda \mathbf{A}_+^\dagger \tilde{\mathbf{S}} \mathbf{A}_- \mathbf{O}_2^\mu) \mathbf{A}_+^\dagger \tilde{\mathbf{S}} \end{aligned} \quad (\text{B19})$$

where only $\tilde{\mathbf{O}}_2^{\mu\lambda}$ is not known. Next, one differentiates eq 1 with regard to the two external parameters μ and λ and, after some algebra, obtains

$$\begin{aligned} \mathbf{O}^{\mu\lambda} \varepsilon - \varepsilon \mathbf{O}^{\mu\lambda} &= (\Phi^\dagger \tilde{\mathbf{D}}^{\mu\lambda} \Phi - \Phi^\dagger \tilde{\mathbf{S}}^{\mu\lambda} \Phi \varepsilon) - \Phi^\dagger \tilde{\mathbf{S}}^\mu \\ & \quad \Phi (\Phi^\dagger \tilde{\mathbf{D}}^\lambda \Phi - \Phi^\dagger \tilde{\mathbf{S}}^\lambda \Phi \varepsilon) - \Phi^\dagger \tilde{\mathbf{S}}^\lambda \\ & \quad \Phi (\Phi^\dagger \tilde{\mathbf{D}}^\mu \Phi - \Phi^\dagger \tilde{\mathbf{S}}^\mu \Phi \varepsilon) \\ & \quad + [(\Phi^\dagger \tilde{\mathbf{D}}^\mu \Phi - \Phi^\dagger \tilde{\mathbf{S}}^\mu \Phi \varepsilon), \mathbf{O}^\lambda] \\ & \quad + [(\Phi^\dagger \tilde{\mathbf{D}}^\lambda \Phi - \Phi^\dagger \tilde{\mathbf{S}}^\lambda \Phi \varepsilon), \mathbf{O}^\mu] \\ & \quad - \mathbf{O}^\mu [\mathbf{O}^\lambda, \varepsilon] - \mathbf{O}^\lambda [\mathbf{O}^\mu, \varepsilon] - \varepsilon^{\mu\lambda} \end{aligned} \quad (\text{B20})$$

where $[a,b] = a \cdot b - b \cdot a$ is a commutator. Because in eq B19 only the off-diagonal part of the operator $\tilde{\mathbf{O}}^{\mu\lambda}$ is needed, the last term $\varepsilon^{\mu\lambda}$ does not make any contribution to it. The diagonal part can be obtained from differentiation of the normalization condition $\Phi^\dagger \mathbf{M} \Phi = \mathbf{I}$ with respect to μ and λ . However, this is not necessary, because $i \neq j$ is always true for $\tilde{\mathbf{O}}_2^{\mu\lambda}$.

According to eq B3, both ε_i and ε_j correspond to the electronic eigenvalues for $(\mathbf{O}_4^\mu)_{ij}$. If ε_i and ε_j ($i \neq j$) are quasi-degenerate or degenerate, the matrix elements $(\mathbf{O}_4^\mu)_{ij}$ may become undetermined by eq B1. Because an orthogonal transformation of the degenerate energy levels leaves the energy unchanged, the undetermined elements of $(\mathbf{O}_4^\mu)_{ij}$ may be set to zero. The derivatives $\partial^2 \mathbf{U} / \partial \mu \partial \lambda$ obtained from eq B19 are contracted with the second derivatives of matrices $\mathbf{S}, \mathbf{T}, \mathbf{V}$, and \mathbf{W} , which were precomputed and saved in lower triangular arrays as described after eq A5.

C. APPENDIX: NESC COUPLED PERTURBED EQUATIONS

The derivatives $\partial \mathbf{P} / \partial \mu$ and $\partial \mathbf{Q} / \partial \mu$ in eq 21 are obtained from the coupled-perturbed (CP) equations.³⁵ The orbital rotation operator \mathbf{O}^μ in eq C1

$$\frac{\partial \mathbf{C}}{\partial \mu} = \mathbf{C} \mathbf{O}^\mu \quad (\text{C1})$$

connects the first derivatives $\partial \mathbf{C} / \partial \mu$ of the molecular orbitals \mathbf{C} with respect to the perturbation μ . Differentiating the SCF equations with the Fock operator 13 with respect to the perturbation, one obtains a set of equations for the elements of the operator \mathbf{O}^μ :

$$\mathbf{O}_{ij}^\mu = \begin{cases} (\varepsilon_j - \varepsilon_i)^{-1} ((\mathbf{C}^\dagger \frac{\partial \mathbf{F}}{\partial \mu} \mathbf{C})_{ij} - (\mathbf{C}^\dagger \frac{\partial \mathbf{S}}{\partial \mu} \mathbf{C})_{ij} \varepsilon_j) & \text{for } i \neq j \\ -\frac{1}{2} (\mathbf{C}^\dagger \frac{\partial \mathbf{S}}{\partial \mu} \mathbf{C})_{ii} & \text{for } i = j \end{cases} \quad (\text{C2})$$

Because the derivative $\partial \mathbf{F} / \partial \mu$ of the Fock operator depends on the first-order orbitals via the first derivative of the density matrix \mathbf{P}

$$\begin{aligned} \left(\frac{\partial \mathbf{F}}{\partial \mu} \right)_{\rho\tau} &= \left(\frac{\partial \mathbf{H}_{1e}}{\partial \mu} \right)_{\rho\tau} + \left(\frac{\partial}{\partial \mu} (\mathbf{J} - \mathbf{K}) \right)_{\rho\tau} \\ &= \frac{\partial (\mathbf{H}_{1e})_{\rho\tau}}{\partial \mu} + \sum_{\nu\sigma} \frac{\partial P_{\nu\sigma}}{\partial \mu} [(\rho\tau|\nu\sigma) - (\rho\sigma|\tau\nu)] \\ &\quad + \sum_{\nu\sigma} P_{\nu\sigma} \left[\frac{\partial (\rho\tau|\nu\sigma)}{\partial \mu} - \frac{\partial (\rho\sigma|\tau\nu)}{\partial \mu} \right] \end{aligned} \quad (\text{C3})$$

Equation C2 needs to be solved iteratively. Having obtained operator \mathbf{O}^μ , the quantities entering eq 21 are calculated as in eqs C4 and C5

$$\frac{\partial \mathbf{P}}{\partial \mu} = \mathbf{C}(\mathbf{O}^\mu \mathbf{n} + \mathbf{n}(\mathbf{O}^\mu)^\dagger) \mathbf{C}^\dagger \quad (\text{C4})$$

$$\begin{aligned} \frac{\partial \mathbf{\Omega}}{\partial \mu} &= \mathbf{C} \left(\mathbf{O}^\mu \mathbf{n} \mathbf{e} + \mathbf{n} \mathbf{e} (\mathbf{O}^\mu)^\dagger + \mathbf{n} (\mathbf{O}^\mu)^\dagger \mathbf{e} + \mathbf{n} \mathbf{e} \mathbf{O}^\mu \right. \\ &\quad \left. + \mathbf{C}^\dagger \frac{\partial \mathbf{F}}{\partial \mu} \mathbf{C} \right) \mathbf{C}^\dagger \end{aligned} \quad (\text{C5})$$

In eq C3, the derivatives $\partial \mathbf{H}_{1e} / \partial \mu$ of the NESC one-electron Hamiltonian are used in matrix form. These derivatives can be obtained using the formalism described in section 3, and the matrices $\partial \mathbf{P} / \partial \mu$ and $\partial \mathbf{\Omega} / \partial \mu$ can be saved for further use in connection with eq 21.

AUTHOR INFORMATION

Corresponding Author

*E-mail: mike.filatov@gmail.com; dcremer@gmail.com.

Notes

The authors declare no competing financial interest.

ACKNOWLEDGMENTS

This work was financially supported by the National Science Foundation, Grant CHE 1152357. We thank SMU for providing computational resources.

REFERENCES

- (1) Dyall, K. G.; Fægri, K. *Introduction to Relativistic Quantum Chemistry*; Oxford University Press: Oxford, U.K., 2007.
- (2) Yamaguchi, Y.; Goddard, J. D.; Osamura, Y.; Schaefer, H. F. S. *A New Dimension to Quantum Chemistry: Analytic Derivative Methods in Ab Initio Molecular Electronic Structure Theory*; Oxford University Press: Oxford, U.K., 1994.
- (3) Dyall, K. G. *J. Chem. Phys.* **1997**, *106*, 9618.
- (4) Dyall, K. G.; Enevoldsen, T. *J. Chem. Phys.* **1999**, *111*, 10000.
- (5) Dyall, K. G. *J. Comput. Chem.* **2002**, *23*, 786–793.
- (6) Filatov, M.; Dyall, K. G. *Theor. Chem. Acc.* **2007**, *117*, 333.
- (7) Zou, W.; Filatov, M.; Cremer, D. *Theor. Chem. Acc.* **2011**, *130*, 633–644.
- (8) Filatov, M. *J. Chem. Phys.* **2006**, *125*, 107101.
- (9) Kutzelnigg, W.; Liu, W. *J. Chem. Phys.* **2006**, *125*, 107102.
- (10) Cremer, D.; Kraka, E.; Filatov, M. *ChemPhysChem* **2008**, *9*, 2510.
- (11) Kraka, E.; Filatov, M.; Cremer, D. *Croat. Chem. Acta* **2009**, *82*, 233–243.
- (12) Kraka, E.; Cremer, D. *Int. J. Mol. Sci.* **2008**, *9*, 926–942.
- (13) Filatov, M.; Danovich, D. *J. Phys. Chem. A* **2008**, *112*, 12995–13001.
- (14) Filatov, M. *J. Chem. Phys.* **2007**, *127*, 084101.
- (15) Kurian, R.; Filatov, M. *J. Chem. Theory Comput.* **2008**, *4*, 278–285.
- (16) Kurian, R.; Filatov, M. *J. Chem. Phys.* **2009**, *130*, 124121.

- (17) Kurian, R.; Filatov, M. *Phys. Chem. Chem. Phys.* **2010**, *12*, 2758–2762.
- (18) Wolf, A.; Reiher, M.; Hess, B. A. *J. Chem. Phys.* **2002**, *117*, 9215.
- (19) Wolf, A.; Reiher, M.; Hess, B. A. *J. Chem. Phys.* **2004**, *120*, 8624.
- (20) Reiher, M.; Wolf, A. *J. Chem. Phys.* **2004**, *121*, 2037.
- (21) Reiher, M.; Wolf, A. *J. Chem. Phys.* **2004**, *121*, 10945.
- (22) Iliaš, M.; Jensen, H. J. A.; Roos, B. O.; Urban, M. *Chem. Phys. Lett.* **2005**, *408*, 210.
- (23) Iliaš, M.; Saue, T. *J. Chem. Phys.* **2007**, *126*, 064102.
- (24) Barysz, M.; Mentel, L.; Leszczynski, J. *J. Chem. Phys.* **2009**, *130*, 164114.
- (25) Kutzelnigg, W.; Liu, W. *J. Chem. Phys.* **2005**, *123*, 241102.
- (26) Kutzelnigg, W.; Liu, W. *Mol. Phys.* **2006**, *104*, 2225.
- (27) Liu, W.; Kutzelnigg, W. *J. Chem. Phys.* **2007**, *126*, 114107.
- (28) Cheng, L.; Gauss, J. *J. Chem. Phys.* **2011**, *135*, 084114.
- (29) Cheng, L.; Gauss, J. *J. Chem. Phys.* **2011**, *135*, 244104.
- (30) Zou, W.; Filatov, M.; Cremer, D. *J. Chem. Phys.* **2011**, *134*, 244117.
- (31) Filatov, M.; Zou, W.; Cremer, D. *J. Chem. Theory Comput.* **2012**, *8*, 875–882.
- (32) Filatov, M.; Zou, W.; Cremer, D. *J. Phys. Chem. A* **2012**, *116*, 3481–3486.
- (33) Filatov, M.; Zou, W.; Cremer, D. *J. Chem. Phys.* **2012**, submitted.
- (34) Liu, W.; Peng, D. *J. Chem. Phys.* **2009**, *131*, 031104.
- (35) Pople, J. A.; Krishnan, R.; B., S. H.; Binkley, J. S. *Int. J. Quantum Chem. Quantum Chem. Symp.* **1979**, *13*, 225–241.
- (36) Kraka, E.; Filatov, M.; Gräfenstein, J.; Zou, W.; Izotov, D.; Gauss, J.; He, Y.; Wu, A.; Polo, V.; Olsson, L.; Konkoli, Z.; He, Z.; Cremer, D. *COLOGNE2011*, 2011.
- (37) Stratmann, R. E.; Burant, J. C.; Scuseria, G. E.; Frisch, M. J. *J. Chem. Phys.* **1997**, *106*, 10175.
- (38) Head-Gordon, M.; Head-Gordon, T. *Chem. Phys. Lett.* **1994**, *220*, 122.
- (39) Adamo, C.; Barone, V. *J. Chem. Phys.* **1998**, *110*, 6158.
- (40) Stevens, P. J.; Devlin, F. J.; Chabrowski, C. F.; Frisch, M. J. *J. Phys. Chem.* **1994**, *98*, 11623.
- (41) Head-Gordon, M.; Pople, J. A.; Frisch, M. J. *Chem. Phys. Lett.* **1988**, *153*, 503.
- (42) EMSL Basis Set Exchange. <https://bse.pnl.gov/bse/portal> (accessed Jun. 2012).
- (43) Pantazis, D. A.; Chen, X.-Y.; Landis, C. R.; Neese, F. *J. Chem. Theory Comput.* **2008**, *4*, 908.
- (44) Tatewaki, H.; Koga, T. *Chem. Phys. Lett.* **2000**, *328*, 473.
- (45) Data base of Segmented Gaussian Basis Sets, Quantum Chemistry Group, Sapporo, Japan. <http://setani.sci.hokudai.ac.jp/sapporo/Welcomedo>.
- (46) Tsuchiya, T.; Abe, M.; Nakajima, T.; Hirao, K. *J. Chem. Phys.* **2001**, *115*, 4463.
- (47) *Accurate relativistic Gaussian basis sets for H through Lr determined by atomic SCF calculations with the third-order Douglas–Kroll approximation*; Advanced Science Institute: Riken, Japan. <http://www.riken.jp> (accessed Jun. 2012).
- (48) Dyall, K. G. Available from the Dirac website: <http://dirac.chem.sdu.dk> (accessed Jun. 2012).
- (49) Visscher, L.; Dyall, K. G. *At. Data Nucl. Data Tables* **1997**, *67*, 207.
- (50) Gabrielse, G.; Hanneke, D.; Kinoshita, T.; Nio, M.; Odom, B. *Phys. Rev. Lett.* **2006**, *97*, 030802.
- (51) Zuev, V. S.; Eden, J. G.; Tran, H. C. *Opt. Spectrosc.* **2001**, *90*, 516.
- (52) Bishea, G. A.; Morse, M. D. *J. Chem. Phys.* **1991**, *95*, 5646.
- (53) Borschevsky, A.; Pershina, V.; Eliav, E.; Kaldor, U. *GSI Sci. Rep.* **2008**, *146*.
- (54) Barber, R.; Gäggeler, H. W.; Karl, P. W.; Nakahara, H.; Vardach, E.; Vogt, E. *Pure Appl. Chem.* **2009**, *81*, 1331.
- (55) Anton, J.; Fricke, B.; Schwerdtfeger, P. *Chem. Phys.* **2005**, *311*, 97.
- (56) Cremer, D.; He, Z. *J. Chem. Phys.* **1996**, *100*, 6173–6188.

- (57) Wang, X.; Andrews, L.; Riedel, R.; Kaupp, M. *Angew. Chem., Int. Ed. Engl.* **2007**, *46*, 8371.
- (58) Konkoli, Z.; Cremer, D. *Int. J. Quantum Chem.* **1998**, *67*, 1–9.
- (59) Cremer, D.; Larsson, J. A.; Kraka, E. In *Theoretical and Computational Chemistry*; Parkanyi, C., Ed.; Elsevier: Amsterdam, 1998; Theoretical Organic Chemistry Vol. 5, p 259.
- (60) Cremer, D.; Kraka, E. *Curr. Org. Chem.* **2010**, *14*, 1524–1560.
- (61) Pickardt, E.; Chrzanowski, L.; Steudel, R.; Borowski, M. *Z. Naturforsch., B: J. Chem. Sci.* **2004**, *59*, 1077–1082.
- (62) Johnson, C. R. *Am. Math. Month.* **1970**, *259*, 77.
- (63) Smith, R. A. *SIAM J. Appl. Math.* **1968**, *16*, 198.
- (64) Xue, J.; Xu, S.; Li, R.-C. *Numer. Math.* **2012**, *120*, 639.
- (65) Zhou, B.; Lam, J.; Duan, G.-R. *Appl. Math. Lett.* **2009**, *22*, 1038.
- (66) Filatov, M.; Cremer, D. *J. Chem. Phys.* **2003**, *118*, 6741.
- (67) Filatov, M.; Cremer, D. *J. Chem. Phys.* **2004**, *120*, 11407–11422.
- (68) Reiher, M.; Wolf, A. *J. Chem. Phys.* **2006**, *124*, 064102.
- (69) Dufayard, J.; Majourat, B.; Nedelec, O. *Chem. Phys.* **1988**, *128*, 537.
- (70) Shayesteh, A.; Yu, S.; Bernath, P. F. *J. Phys. Chem. A* **2005**, *109*, 10280.
- (71) Pyykkö, P.; Straka, M.; Patzschke, M. *Chem. Commun.* **2002**, *38*, 1728.
- (72) Huber, K. P.; Herzberg, G. *Molecular Spectra and Molecular Structure IV. Constants of Diatomic Molecules*; Van Nostrand Reinhold: New York, 1979.
- (73) Kim, J.; Ihee, H.; Lee, Y. S. *J. Chem. Phys.* **2010**, *133*, 144309.
- (74) Rai, A. K.; Rai, S. B.; Rai, D. K. *J. Phys. B: At. Mol. Phys.* **1982**, *15*, 3239.
- (75) Okabayashi, T.; Nakaoka, Y.; Yamazaki, E.; Tanimoto, M. *Chem. Phys. Lett.* **2002**, *366*, 406.
- (76) Jackson, V. E.; Craciun, R.; Dixon, D. A.; Peterson, K. A.; de Jong, W. A. *J. Phys. Chem. A* **2008**, *112*, 4095.
- (77) Zhou, M.; Andrews, L.; Li, J.; Bursten, B. E. *J. Am. Chem. Soc.* **1999**, *121*, 9712.
- (78) Cao, X.; Dolg, M.; Stoll, H. *J. Chem. Phys.* **2003**, *118*, 487.